Laboratory of Geo-Information Science and Remote Sensing

Thesis Report GIRS-2018-01

Remote Sensing for Date Production

Time series analysis for date plantation monitoring

Rob Maas

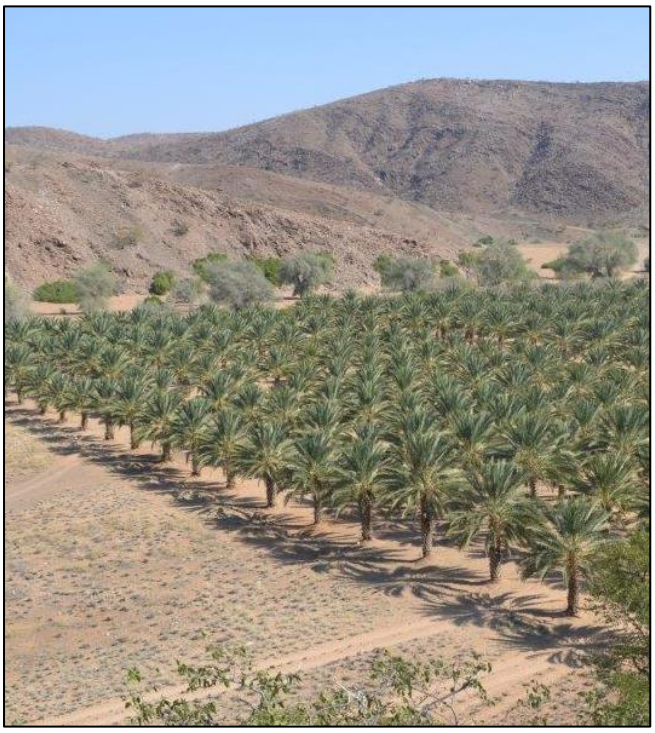

January 2018

WAGENINGEN UNIVERSITY
WAGENINGEN UR

Remote Sensing for Date Production

Time series analysis for date plantation monitoring

R.C. Maas

Registration number 89 07 12 537 130

Supervisors:

Lammert Kooistra
Steven Wonink (eLEAF)

A thesis submitted in partial fulfilment of the degree of Master of Science
at Wageningen University and Research Centre,
The Netherlands.

January 23, 2017
Wageningen, The Netherlands

Thesis code number: GRS-80436
Thesis Report: GIRS-2018-01
Wageningen University and Research Centre
Laboratory of Geo-Information Science and Remote Sensing

Cover image: Namibia Development Corporation (2018)

Summary

Dates play a key role in the diet of Middle-Eastern and Northern African countries, as they are one of the few sources of vitamins and minerals that can be cultivated in the arid regions. Modernization of the date sector is needed to cope with the growing demand and the challenges they face, such as water scarcity, salinization and pest control. The aim of this study is to aid the date farmers by exploring a new monitoring tool: satellite remote sensing.

Three time series analyses were performed on Landsat 7 NDVI signals to investigate two farms, a modern 'model' and a traditional 'standard' farm. Firstly, the interannual signals of several fields were investigated for their differences and their sensitivity to varying weather. Secondly, the average seasonal pattern of each field was calculated to find correlations with farm operations. Thirdly, the heterogeneity within each field was calculated to identify fields that contain bad regions. Furthermore, the outcomes of these analyses were visualized in accessible maps that can show the state of the fields at once, without requiring any specific knowledge.

The following conclusions were drawn from the research: (i) Landsat 7 NDVI signals are the most sensitive to vegetation changes and could not be used with Landsat 8 NDVI data. (ii) The NDVI signals of the different fields follow logical and distinct patterns. They also show interannual growth and harvesting operations are detectable. But the signals are unaffected by weeding, precipitation and temperature. (iii) Both farms are characterized by different types of time series; the model farm shows parallel and regular signals, whereas the standard farm is irregular and has large differences between the fields. (iv) To best aid the farmers it is essential to provide accessible information, therefore the time series analysis outcomes were visualized in clear maps. The main recommendation for future work is that more plantation operational information and yield data are needed to validate whether the time series variations correlate with actual plantation performance.

Contents

Summary **V**

1 Introduction **1**
1.1 Background 1
1.2 Problem Description 2
1.3 Objective and Research Questions 4
1.4 Outline Report 5

2 Background Literature **7**
2.1 Date Cultivation 7
2.2 Time Series Analysis 8
2.2.1 Vegetation Monitoring 8
2.2.2 Analysis Methods 9

3 Study Area and Data Description **11**
3.1 Study Area 11
3.1.1 Al-Kharj governorate 12
3.1.2 Model and Standard Plantations 12
3.2 Data Description 13
3.2.1 Satellite Imagery 13
3.2.2 Meteorology Data 15
3.2.3 Farm Management Information 15

4 Methodology **17**
4.1 Downloading and Preprocessing Imagery 17
4.2 Vegetation Index Calculation 19
4.3 Satellite and Vegetation Index Comparison 19
4.4 Mean NDVI Mapping and Subset Fields 20
4.5 Interannual Trend Analysis 20
4.6 Seasonal Pattern Analysis 21
4.7 Heterogeneity Analysis 21

5 Results **23**
5.1 Plantation Performance Indicators . . . 23
5.2 Interannual Analysis . . . 26
5.3 Seasonal pattern . . . 29
5.4 Heterogeneity analysis . . . 32

6 Discussion **37**
6.1 Plantation Performance Indicators . . . 37
6.2 Interannual Analysis . . . 38
6.3 Seasonal Analysis . . . 39
6.4 Heterogeneity Analysis . . . 40
6.5 Satellite Monitoring Potential . . . 40

7 Conclusions & Recommendations **43**
7.1 Conclusions . . . 43
7.2 Recommendations . . . 43

Acknowledgements **44**

Bibliography **50**

Appendices **52**
A Plantation Calendar . . . 52
B Additional Results . . . 55
B.1 NDVI versus SAVI . . . 55
B.2 LandSat 7 versus LandSat 8 . . . 56
B.3 Interannual Analysis . . . 58
C USB Memorystick Content . . . 58

1 Introduction

This chapter will describe the background of date production before moving to the problem description and the objectives of this research. Finally, the outline of this report is described.

1.1 Background

Dates (*Phoenix dactylifera*) are eaten all over the world and play a key role in the daily diet of Middle-Eastern and Northern African countries (Figure 1.1). They are being cultivated in all arid areas between Morocco and India, because of their high resilience for water stress (Chao and Krueger 2007). Historically, dates are important in different socio-economic fields in these regions, where they have been consuming dates for 6000 years (Zohary 2000). Caravan routes emerged just for the transportation of dates, and in the Babylonian and Assyrian times the cultivation of dates was considered a sacred symbol of fertility (Chao and Krueger 2007).

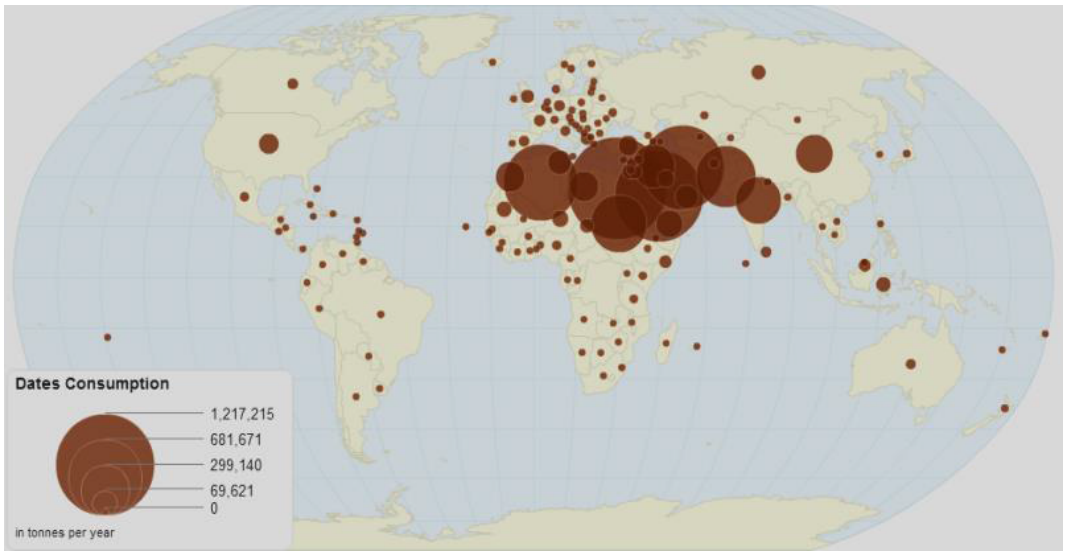

Figure 1.1: Date consumption per country (Source: (FAO 2012)).

Dates contribute much to the public health of the Middle East and North Africa as 90% is consumed locally and they contain much nutrients, such as vitamins, proteins and minerals (Zaid et al. 2002b). The inedible parts of the trees are used for roofs, brooms and fishing boats, among other things (Johnson 2016). Therefore, the Food and Agriculture Organization (FAO) of the United Nations (UN) has recognized the social, economic and ecological importance of date cultivation for a long time (Arias, Hodder, and Oihabi 2016). But even though the FAO is engaged in developing the cultivation methods for over 70 years, there are many reasons for concern.

1.2 Problem Description

Worldwide date production has more than tripled between 1962 and 2005 because of the growing world population and the increasing demand of dates for exportation (FAO 2012). With the projected growth of the world population, the date demand will only continue to grow in order to supply the growing population in arid regions with a source of nutrients (United Nations 2015). When trying to meet the growing demands and increase the production, farm managers are confronted even more with difficult challenges they already face, like water management, salinization and pest control.

Many date plantations still used flood irrigation, meaning that large amounts of water are released at once to cover parts of a plantation with a layer of water (Al-Karaki 2013). The roots then extract water from the infiltrating water. This type of irrigation is easy to apply and relatively cheap. However, with this technique much of the water infiltrates deep into the sandy soil or evaporates before it gets extracted by the roots resulting in a low water use efficiency (Zaid et al. 2002b; Abdul Salam and Al Mazrooei 2006). Due to the water scarcity in arid regions it is important to increase the efficiency, especially in the Kingdom of Saudi Arabia water availability is a serious problem as most of its water comes from a fossil aquifer (Al-Ibrahim 1991), and the aquifer is depleting quickly (Gazette 2016). Therefore, it is wise to invest in more sophisticated and efficient irrigation techniques like drip irrigation (Al-Amoud 2006).

Salinization is another difficult and expensive problem the farmers face. The minerals in the large quantities of water that are used for irrigation accumulate in the soil, reaching levels that are not tolerated by the date palms (Haj-Amor et al. 2016). Early detection of salt stress in the palms and monitoring of salt levels in soils is essential to deal with salinization in time (Allbed, Kumar, and Sinha 2014).

Another challenge date farmers face is pest control. Currently the Red Palm Weevil (RPW), *Rhynchophorus ferrugineus*, is causing severe economic and biological damage. The larvae of the RPW dig holes in the trunk of the palms that sever the veins, resulting in a reduced production or even the death of a palm (Gutiérrez et al. 2010; Gush 1999). The RPW outbreaks has long been ignored, so it could spread across the continent and is now an international problem for the date sector (Giblin-Davis 2001).

Modernization of the date cultivation sector is needed to cope with the growing demand and face the growing problems caused by water shortage, salinization and pests. Improving the plantation monitoring is an important step in this process. Closely watching the palms is necessary to act quickly when the trees require additional attention, e.g. adjustment of the water supply of the drip irrigation or starting pest control. Remote sensing can be a valuable tool for the plantation managers, as this provides them with additional information about the entire farm. Using Unmanned Aerial Vehicles (UAVs) or aeroplanes to regularly survey the plantation has proven to be effective and successful (Shendryk et al. 2016; Y. Cohen et al. 2012), but is still too costly for most farm managers. Therefore, this study explored the potential of using satellite remote sensing to monitor date plantations. This would be a valuable tool for farmers, also by opening up opportunities for regional monitoring. Managers would be able to compare the biomass development and yield of their plantation with others in the region, revealing how well they perform and whether improvements could be made. Furthermore, authorities could use regional information to make better informed decisions, e.g. about water distribution and logistics. Especially with the continuous improvements of satellites this will be more and increasingly feasible.

Satellite remote sensing has been used to study and monitor vegetation for decades (Running 1986; Prince and Astle 1986; Iverson, Graham, and Cook 1989). With the newer non-commercial satellites, such as LandSat 8 and Sentinel-2, the resolutions are high enough to use them as farming tools. The spatial resolutions allow monitoring at sub-field level and the revisit time is short enough to have frequent survey moments. Previous studies that use satellite imagery for agricultural purposes show promising results for yield estimation (Xin et al. 2013; Chivasa, Mutanga, and Biradar 2017; Lobell, Thau, et al. 2015), estimate irrigation requirements (Toureiro et al. 2017) and monitor soil salinity (Gorji, Sertel, and Tanik 2017). However, threats like water stress of pest outbreaks are not directly detectable from satellite images, so a vegetation index (VI) was used as a proxy for date palm health and performance. A VI utilizes the spectral response of two or more bands to quantify the terrestrial photosynthetic activity within a pixel (Alfredo Huete et al. 2002). The Soil Adjusted Vegetation Index (SAVI) was used in an earlier study by Alhammadi and Glenn (2008) to monitor date palm health in the United Arab Emirates, using satellite imagery. However, their research focussed on the long-term change of entire regions, so they only compared two images from 1987 and 2000. This study is aimed at exploring a tool for individual plantations, thus a higher spatial and temporal resolution is required to be of added value to the farmers. Therefore, time series analysis on the VI values is conducted to study the temporal behaviour of the vegetation throughout the years. Different fields within a plantation are compared to determine if satellites are capable of detecting vegetation variations that correlate with events that occur within the date plantations. However, many vegetation indices exist and they all have different advantages and applications (Alfredo Huete et al. 2002).

Therefore, the first step of this study was to investigate which VI would be most suited for monitoring date plantations.

For this study it was required that the satellite imagery accommodates high spatial and temporal resolutions to detect gradual changes at sub-field level scale. Moreover, multiple years of data has to be available for the time series analysis, so years can be compared and interanual trends can be detected. The Sentinel-2 constellation provides high resolution data that is available for free, but these two satellites were launched on 23 June 2015 and 7 March 2017, so they have not been operational long enough to provide a long time series(ESA 2018). On the other hand, the Landsat 7 and Landsat 8 satellites were launched at 15 April 1999 and 11 February 2013, respectively (USGS 2018). Furthermore, the imagery of both these satellites is freely available and possesses the required resolutions, and was therefore chosen as input data for this study. Both Landsat satellites have a revisit time of 16 days, but the temporal resolution could in theory be doubled by combining the images so the revisit frequency is once every 8 days. However, because the satellites contain different sensors it cannot be guaranteed that there is no offset in the produced vegetation index values (Xu and Guo 2014). This was therefore also investigated at the start of the research.

1.3 Objective and Research Questions

The aim of this study is aid the date farmers in the middle-east by exploring a new monitoring tool. Although satellite images cannot distinguish individual palms, if satellite monitoring shows good potential it could be incorporated in a larger system where its role could be to identify anomalous areas that require further inspection. Such a tool would help the farmers to better cope with the challenges that the vastly increasing demand in dates present. Additionally, such a tool will provide government officials with more and accessible data, so they can make better informed decisions regarding issues like water distribution. In short, the objective of this study is;

To explore the potential of using satellite imagery for monitoring date plantation.

The following research questions were addressed to achieve the objective:

1. What data and vegetation index is best suited for date performance monitoring?
2. Do the temporal characteristics of the vegetation index show variations that can be related to farming operations and other external influences?
3. Do different farm management techniques, modern compared to traditional, result in detectable differences in the vegetation index time series?
4. How can the time series information be used by the farmers?

1.4 Outline Report

Background literature to support this report is presented in Chapter 2, it contains information that can aid in interpreting the results, understanding the methodology and placing the study in a scientific context. An in-depth description of the study area is presented in the same chapter that provides detailed information about the data that was used, namely Chapter 3. Chapter 4 features the methodology that was followed to answer the research questions and achieve the objective. The results that are presented in Chapter 5 follow only partly the order of the research questions, but this will become apparent in the methodology. The results will be discussed in Chapter 6, where also recommendations for future research are given. Finally, the conclusions of this research are featured in Chapter 7.

2 Background Literature

The purpose of this chapter is to provide additional information to support this report. It contains background information on date cultivation, which can aid in interpreting the results of this study. Furthermore, research that used time series analysis to study vegetation is presented to provide scientific context and support the methodology.

2.1 Date Cultivation

Date palms require hot, dry and long summers to grow, making them very suitable for arid regions where hardly any other nutritious vegetation can grow. (Chao and Krueger 2007). Date palms require a minimal temperature of at least 18 degrees centigrade to start flowering and the optimal temperature for date palm growth is between 32 and 40 degrees centigrade. Date palms do not tolerate rain or humid air while ripening, but require large quantities of groundwater to reach their potential yield (Y. Cohen et al. 2012). These conditions were naturally only found in oases in the desert, but have been artificially created using irrigation.

Date palms have a yearly cycle and can be harvested each year. The trees mature at age 10–15 and bear fruits for well over 100 years. During the relative cold winter new leafs are developing at the highest point. Meanwhile, the older leafs at the bottom are being pruned, up till April. Male trees produce pollen and female trees the flowers that grow into the dates. From February the pollination process starts, this is done manually as birds and insects are not attracted to the flowers and wind pollination is too unreliable (Robinson, Brown, and Williams 2002). For this reason, plantations only have one or two fields that contain male trees. Once the palms have been flowered and the fruits start to grow, the fruit strands have to be thinned regularly. This is done until the dates are harvested and ensures that the remaining fruits grow bigger (Robinson, Brown, and Williams 2002; Zaid et al. 2002a). The time from flowering to harvesting can vary between 120 and 200 days, depending on the species (Zaid et al. 2002a). Furthermore, regular weeding has be to be carried out under the trees as weeds can grow in the shade of the palms where they also consume irrigation water. The fruits are fully ripened and ready for harvesting at the end of the summer. After the date harvest in October the pruning of fronds starts again, which is the removal of dead or dying leafs.

2.2 Time Series Analysis

A time series is defined as a sequence of observations taken sequentially in time. Typical for a time series is that adjacent observations are dependent. Time series analysis encompasses techniques for analysing this dependence (Box et al. 2015). Time series analysis is very suited when studying vegetation using satellite remote sensing, as there are many years of imagery available. This section presents some past research that has used time series analysis and was helpful for this study.

2.2.1 Vegetation Monitoring

Satellite imagery has been used to monitor vegetation for decades, back in the seventies scientists already used the first LandSat satellite to monitor forests for land-use changes (Aldrich 1975; Robert 1975). The research typically consisted of comparing two images to detect changes in forest extents, first done by visual interpretation and later successfully carried out by computers (Coppin and Bauer 1995; Collins and Woodcock 1996). With the increasing awareness of climate change in the nineties, scientist also became more interested in temporally high-resolution data, e.g. to study changes in growing season lengths (Zhou et al. 2001; Jonsson and Eklundh 2002). Furthermore, high resolution vegetation data of large areas became in high demand for carbon modelling (Goward et al. 2008; Turner et al. 2007).

Monitoring of agricultural crops is now very feasible with the advances that have been made in satellite development. The spatial resolution of the latest satellites allow sub-field level analysis and the high temporal resolutions allow scientists to study the behaviour of the crops throughout a growing season. They analyse the time series and draw conclusions from the patterns of the signals, e.g. about the phenology or performance of the crops. This can be used for improved methods of classification, as was done by Zhang et al (2016). They automatically classified crops in China, based on their phenological behaviour. Time series analysis has also been used by Ren et al (2017) to study corn and soy bean crops in Midwestern U.S. They analysed 8 years of 16-day MODIS EVI data and derived the start and end of the growing seasons with a RMSE of approximately 5 days. These dates are important for farm management and planning, but also for other research, e.g. climate studies (Tao et al. 2006) and improving yield estimates (Bolton and Friedl 2013). Fernandes et al. (2017) also used time series analysis on MODIS NDVI data to successfully predict the sugarcane yield in Sao Paulo State, Brazil, achieving a lower RMSE than the official data surveys. They analysed three years of data to derive 20 metrics that are related to the NDVI curve throughout the growing season. A neural network was trained to estimate yield from these 20 metric values. Veloso et al (2017) used Sentinel NDVI and SAR backscatter time series to study several crops in France and found good correlations with biomass.

Previous studies that used satellite imagery to analyse palms primarily focussed on oil palm plantations, besides the study by Alhammadi and Glenn (2008) that was featured in the introduction. Balasundram et al. (2013) successfully estimated yields on a Malaysian oil palm plantation from a single high resolution QuickBird image. They used linear regression to find a relation between vegetation indices and yield data. Morel et al. (2011) also used regression to find a relation between aboveground biomass and HV-polarized ALOS PALSAR data. They used eight 100meter resolution images from September and October 2008. Synthetic Aperture Radar (SAR) data was also used by Dong et al. (2015), who used yearly PALSAR data to create a time series of the backscatter response. They used these to monitor Indonesian acacia plantations and detect palm oil plantations. Chong et al. (Chong et al. 2017) gives an overview of other remote sensing applications for oil palm plantations. None of these studies make use of time series analysis to analyse the phenology of the palms throughout the growing season, which is a major added value of my research.

2.2.2 Analysis Methods

Analysis of the time series can be done using different methods, depending on the application. Detection of sudden changes requires other techniques than is needed for yield estimation or field performance monitoring. Abrupt changes in vegetation can be detected using methods like BFAST (Verbesselt et al. 2010). BFAST was used by De Vries et al (2015) to detect deforestation in Ethopia and by (2016) to investigate water storage in China. Wavelet analysis (Sakamoto et al. 2005) was applied to detect land-use changes with an overall accuracy of 94% by Galfod et al (2008). Contextual time series change detection (Chen et al. 2013) is a method that monitors time series that have similar temporal behaviour, e.g. all pixels within a field, for diverging signals.

However, if the application does not require automated detection it can suffice to do the comparison through visual inspection. Especially if the amount of time series that have to be analysed is limited or the area that has to be monitored is large, a visual representation is desired. A typical approach would be to plot the time series values in the same figure and construct trend lines for better visualization and easier interpretation. A trend line is constructed by smoothing the data using regression and can be done in two different way, parametric and non-parametric (Figure 2.1). A parametric regression model fits a line through the points in a scatter plot using a predefined formula, e.g. linear, quadratic, polynomial or sinusoidal (Bianchi, Boyle, and Hollingsworth 1999). The resulting trend lines can then be described using the formula and fitting parameters, and can also conveniently be compared to determine the interanual trend for example. However, a sinusoidal trend line will have the same amplitude and wave length every year, resulting in bad fits when used for vegetation that are expected to have year-to-year variation in their cycle.

The non-parametric regression methods do not have a predetermined form for the trend line. The local regression (LOESS) approach is such a method and was used in this research to plot trend lines. It was designed by Cleveland (1979) and further developed by Cleveland and Devlin (1988). The curve is constructed by fitting a polynomial function at every data point, where only a subset of surrounding data is used. Furthermore, the polynomial fit is done using weighted least squares, so the nearest points have more weight than points further away. The amount of points that are used in the subset is controlled by the span parameter α and is set by the user. A high value means that the polynomials are fitted through many points, while a low α-value results in fits through a smaller number of points, thus resulting in a wigglier line. The advantage of using LOESS is that it is very flexible, as it also works if the time intervals between the points is not equal. This is convenient when working with satellite data and some images have to be omitted due to clouds. A disadvantage is that the method can be computationally demanding because a polynomial function has to be fitted for every data point.

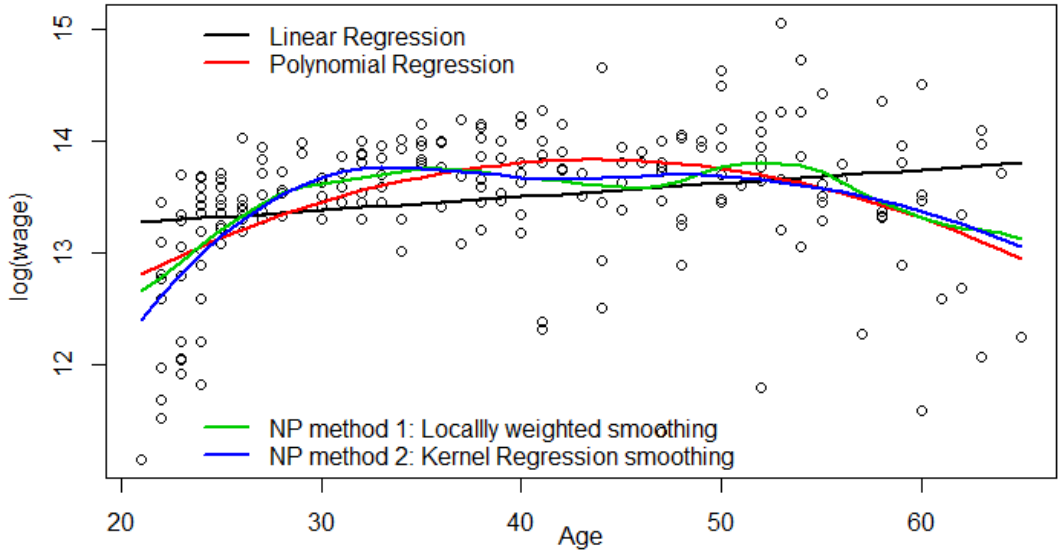

Figure 2.1: Different types of regression lines. The blue and red lines are fitted using a parametric model, while the green and blue lines are non-parametric. (Source: Virginia Tech - Department of Statistics (2018)).

3 Study Area and Data Description

This chapter consists of two sections; the first section describes the study area and the second section presents detailed information about the data that was used for this research.

3.1 Study Area

While the outcome of this study is aimed to aid the entire date sector, this study will focus on the Kingdom of Saudi Arabia (KSA). KSA is the third largest date producing country worldwide, after Egypt and Iran (Table 3.1). After the oil industry, the date industry is the most profitable sector of the Saudi Arabian economy. Plantations in KSA have been dealing with Red Palm Weevil outbreaks since 1987 (Atwa and Hegazi 2014). Furthermore, the country is dealing with an increasing freshwater shortage due to a depleting aquifer (Al-Ibrahim 1991; Gazette 2016). Therefore, the KSA would benefit much from modernization of its agricultural sector and date plantations, and thus is very suited to be the study area. A date plantation in the Al-Kharj governorate has been found willing to participate in multiple scientific studies and will also play a key role in this research by sharing information about the farm operations.

Table 3.1: Date production in 2013 of the five most producing countries and their relative portion of the world date production (FAO 2012)

Country	Production [*10^6kg]	Share of world production [%]
Egypt	1502	18.3
Iran	1084	13.2
Saudi Arabia	1065	13.0
Algeria	848	10.3
Iraq	676	8.2

3.1.1 Al-Kharj governorate

The Kingdom of Saudi Arabia is divided into thirteen regions, which are split into separate governorates. The Al-Kharj governorate is part of the Riyadh region and is located 50km south-east of the national capital Riyadh (Figure 3.1). It is considered the most important agricultural governorate of the KSA, producing dates, cereals, vegetables and fruits (Modaihsh et al. 2015). The region is also known for its dairy production and livestock rearing (Al-Zahrani et al. 2016). The governorate depends on groundwater for its water supply and is therefore susceptible for water scarcity when the fossil aquifer depletes (Al-Omran et al. 2016).

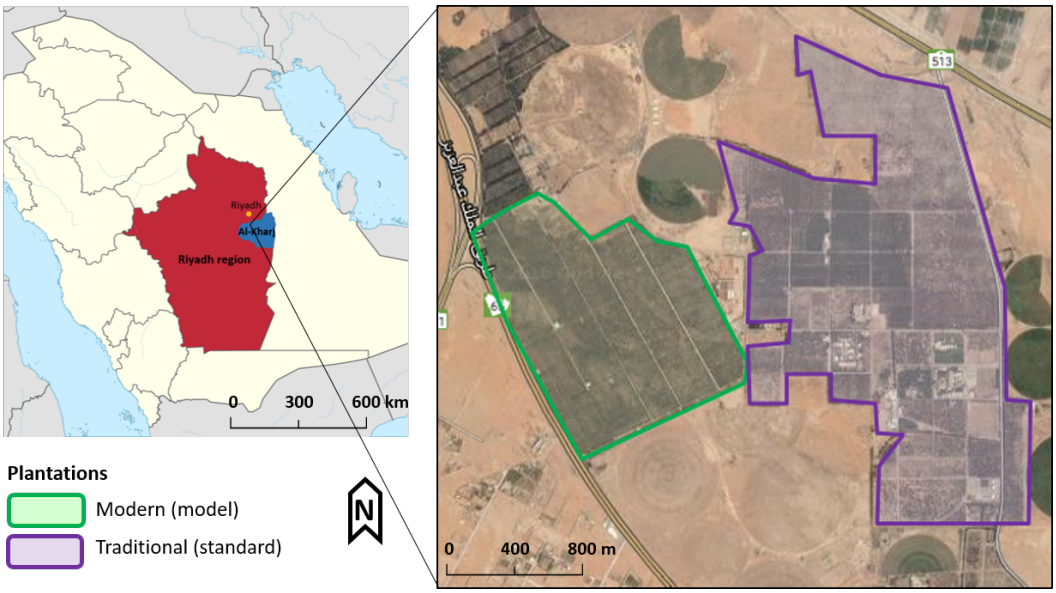

Figure 3.1: The study area of this research. The left map shows the Riyadh region (red) and Al-Kharj governorate (blue) in the Kingdom of Saudi Arabia (Source: Wikipedia). The right image shows the study plantations with the modern and traditional farms highlighted with green and purple, respectively (Source: Google Maps).

3.1.2 Model and Standard Plantations

The two study farms for this research are located at the north-western part of the Al-Kharj agricultural region (Figure 3.1). The plantations are both date plantations, but they differ in management style. The 'standard' farm is a plantation that uses traditional farming and management methods, this farm represents the vast majority of the date plantations in the KSA and the global date sector. The Al-Mohamadia plantation is the 'model' farm, which has switched to modern techniques since a new manager took over in 2013. The plantation has now a strict weeding regime where everything is removed. Furthermore, the farm switched to drip irrigation and every tree now receives water straight to its roots, resulting in less underbrush and more sustainable use of water.

This is also the farm that has shared operational information for research (section 3.2.3). Both study farms are organised into uniform fields that are separated by sandy roads, the model farm uses these blocks as management units for their farming operations.

3.2 Data Description

Data from three different sources was used for this research; LandSat satellite imagery, meteorology data and information about the management activities on the model farm.

3.2.1 Satellite Imagery

Data from two sensors was used in this research, namely Enhanced Thematic Mapper Plus (ETM+) aboard LandSat-7 and the Operational Land Imager (OLI) sensor aboard the LandSat-8 satellite. All available images between February 2009 and February 2017 were downloaded. However, as LandSat-8 became operational in 2013, there is only LandSat-7 data available before that. The imagery was downloaded at processing level 2A using the USGS Glovis portal (http://glovis.usgs.gov) and WRS-2 coordinates p165r43 were used to select the tile containing the study area. The data was processed to surface reflectance using algorithms developed by NASA. LandSat-7 data was processing using LEDAPS, the Landsat Ecosystem Disturbance Adaptive Processing System (Schmidt et al. 2013). LandSat-8 correction was performed using LaSRC, Landsat Surface Reflectance Code (Vermote, Justice, et al. 2016). LaSRC is an extension of the 6SV radiative transfer model (Vermote, Tanré, et al. 1997), using the relatively narrow bands of the OLI-sensor. More technical specifications of the sensors aboard LandSat-7 and LandSat-8 are given in Tables 3.2 and 3.3, respectively.

Table 3.2: Technical specifications of the ETM+ pushbroom sensor aboard LandSat-7.

Product type	Level 2A
Data type	16-bit unsigned integer
Output format	GeoTIFF
Pixel size	15m panchromatic
	30m multispectral
	30m(resampled from 100m) thermal
Map projection	UTM (Polar Stereographic for Antartica)
Datum	WGS 84
Orientation	North-up (map)
Resampling	Cubic convolution
Geometric accuracy	30-50m error, 95 percent confidence
Coverage frequency	Every 16 days
Cross-track field of view	185km

Table 3.3: Technical specifications of the OLI and TIRS-pushbroom sensors aboard LandSat-8.

Product type	Level 2A
Data type	16-bit unsigned integer
Output format	GeoTIFF
Pixel size	15m panchromatic
	30m multispectral
	30m(resampled from 100m) thermal
Map projection	UTM (Polar Stereographic for Antartica)
Datum	WGS 84
Orientation	North-up (map)
Resampling	Cubic convolution
Accuracy	OLI: 12m circular error, 90% confidence
	TIRS: 41m circular error, 90% confidence
Coverage frequency	Every 16 days
Cross-track field of view	190km

3.2.2 Meteorology Data

Meteorology data was used to investigate if detected variations in the date palm performance could be correlated to weather circumstances. Historical weather data was obtained from the History+ service of Meteoblue (www.meteoblue.com). This commercial service provides hourly simulated weather data and covers the entire globe at 30km spatial resolution. For this study we obtained the precipitation and daily maximum temperature for years 2010 – 2017. More detailed information about their weather simulation model can be found on their website (Meteoblue 2017).

3.2.3 Farm Management Information

The farm manager provided detailed information about the farming activities. Appendix A presents the full schedule that show what is done each month in terms of weeding, harvesting, pruning, fertilization and pest control. This schedule was used for the date cultivation section in chapter 2. Furthermore, the amount of water that is being irrigated was provided by the farm manager (Figure 3.2). The fields divided in three groups that receive different amounts of water, based on their age. This information provided helpful context about the ground activities that could be linked to changes in the spectral response of the palms.

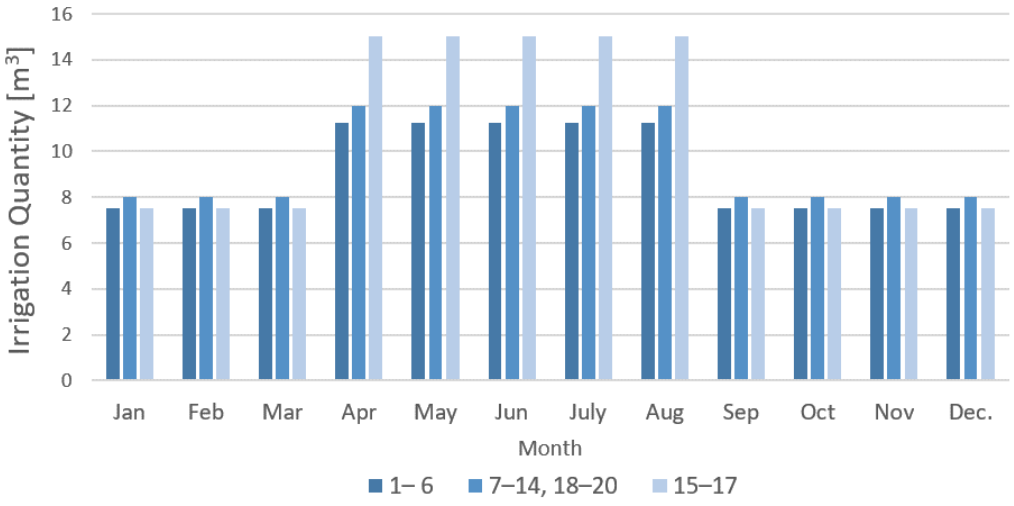

Figure 3.2: Amount of irrigation water that each tree on the model farm receives per month. The fields are divided into three groups that receive different quantities.

4 Methodology

Working out the objective and answering the research questions was done using the methods described in this chapter, first a short summary is given, followed by a visual overview and a step-by-step in-depth description of the methodology.

To determine what data source and vegetation index can best be used to monitor date plantations, I compared the signals from LandSat7 and LandSat8 as well as two vegetation indices. The results from this step answers the first research question and was used for the remainder of the research. To investigate the potential of satellite monitoring I then used time series analysis to look at three properties of the plantation to see if distinct features could be detected in different fields. The characteristics that were investigated were the interanual signal, the seasonal pattern and the amount of heterogeneity within and between fields. These findings answer the second research question. To answer the third research question I also applied the same analysis on the neighbouring, traditional plantation to determine if similar features can be detected there. This methodology is visualized in a flowchart in Figure 4.1 and each of the steps is discussed in more detail as a separate section in this chapter. The processing, analysis and plotting was mostly done using the R scripting language and the scripts can be found on the accompanying USB memory drive and in the following github repository: `https://github.com/Boonalds/MGI_Thesis_Scripts/`.

4.1 Downloading and Preprocessing Imagery

All available LandSat imagery, both LandSat 7 and LandSat 8, for the period 01/01/2007 – 01/05/2017 was downloaded at level-2A processing level from the USGS GloVis portal, more details about the data and sensors are described in section 3.2. This resulted in 149 LandSat 7 images and 99 LandSat 8 images. Further pre-processing was done by cropping the images to the extent of the study farms and by masking all cloud and shadow pixels using the Quality Assessment (QA) band. All pixels that contained a cloud with medium or high confidence were removed from the dataset by assigning NA's to them. So only pixels with bitvalues 1,66,68,72,80,96,112 for LandSat 7 and values 1, 322, 324, 328, 336, 352 and 368 for LandSat 8 were kept for further analysis.

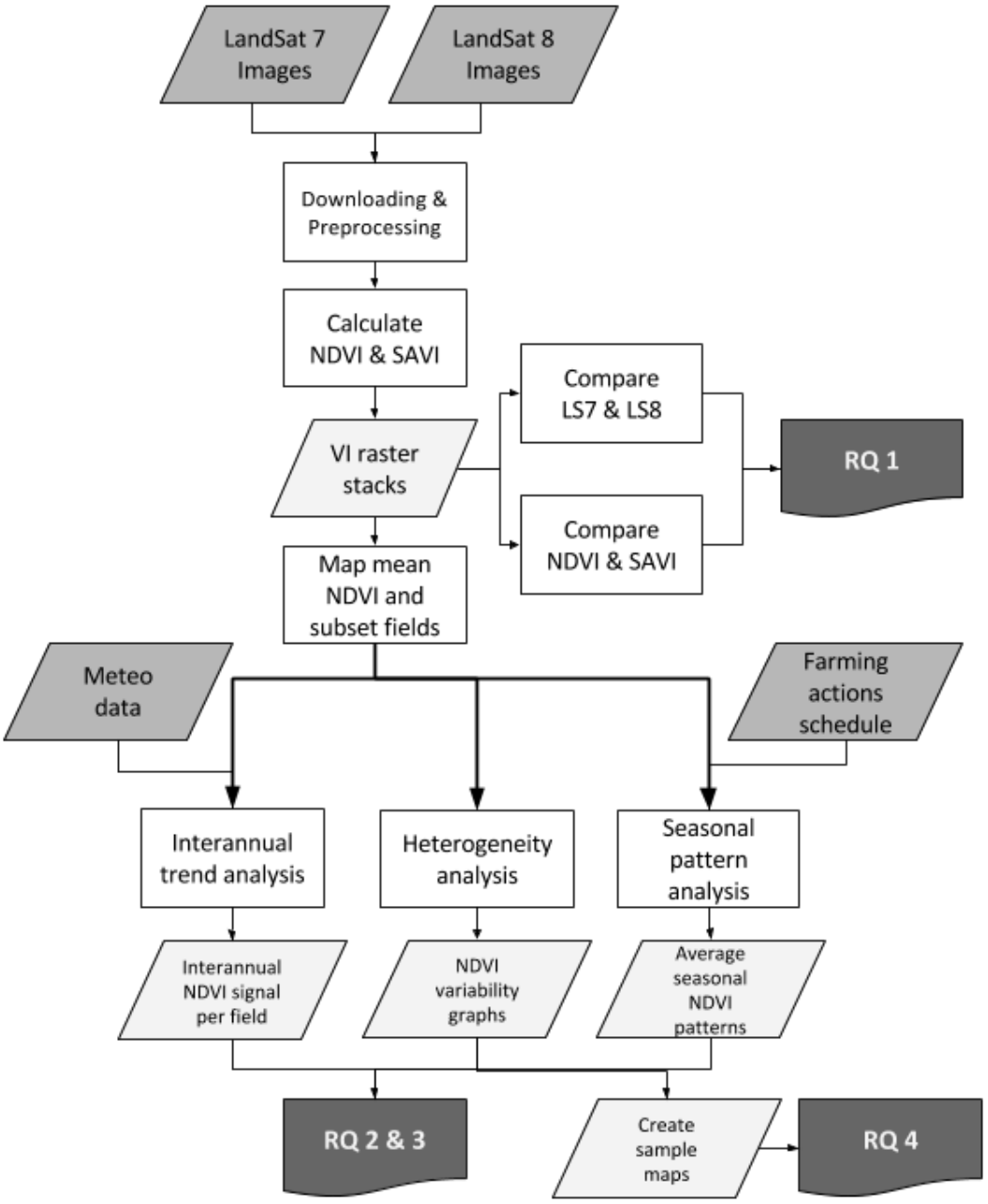

Figure 4.1: Visualization of the methodology that was followed in this study, the steps are described in more detail in the remainder of this chapter.

4.2 Vegetation Index Calculation

The popular and widely used Normalized Difference Vegetation Index (Rouse Jr et al. 1974) (NDVI) was chosen to represent the date palm tree performance. But as the date palms are located far from each other, it was expected that much of the bare soil is detected by the satellite sensors. For this reason it was hypothesized that the Soil Adjusted Vegetation Index (AR Huete 1988) (SAVI) could be more accurate, as this index aims to correct for bare soil reflectance. To investigate whether either one of these indexes would be better suitable for monitoring the plantation, both the NDVI and SAVI values were calculated for each pixel, according to equations 4.1a and 4.1b, respectively. The created NDVI and SAVI maps were stored in convenient rasterstacks for easy processing.

$$NDVI = \frac{(R_{NIR} - R_{Red})}{(R_{NIR} + R_{Red})} \tag{4.1a}$$

$$SAVI = \frac{(1 + L)(R_{NIR} - R_{Red})}{(R_{NIR} + R_{Red} + L)} \tag{4.1b}$$

where R_{Red} and R_{NIR} are the reflectance in the visible red and near-infrared part of the electromagnetic spectrum, respectively. L is a canopy background adjustment factor, that is assumed to be 0.5, which typically results in good estimates (AR Huete 1988).

4.3 Satellite and Vegetation Index Comparison

The next step was to investigate the differences between using NDVI and SAVI as vegetation index to see which one is more useful for monitoring. To do this I calculated for each image the mean NDVI and SAVI values of every field within the plantation, using shapefiles that define the field borders. The two indices were then plotted against the time and in the same figure. Trend lines were fitted so the two indices could be compared better. The trend lines were constructed using the LOESS method, which is described in more detail in section 2.2.2. A span-parameter of 0.15 was used for all trend lines in this study, so the trend line is flexible enough to show variations that occur within the growing season. It was decided to only use NDVI as vegetation index for the further analysis, based on the results that are presented in section 5.1.

Furthermore, it was determined whether the images of LandSat 7 and LandSat 8 could be used together to enhance the temporal resolution, or that it would be better to only use images from one of these sources. To do this, the mean NDVI values per field were calculated for each image. Then the value of both satellites were plotted against time in the same graph, including a LOESS trend line. Histograms of the NDVI value distributions were made for each satellite as well.

4.4 Mean NDVI Mapping and Subset Fields

I decided that I needed to make a selection of fields to investigate further. There are 21 fields located in the model farm and the neighbouring plantation contains 65 fields, which is too much to investigate properly. First of all, because it makes the figures unreadable when there are over 60 lines in there. Secondly, because not every field is representative for the farm it is in. Some fields only contain male palm trees that are being used for pollination, while for some fields in the standard farm it is doubtful that they contain trees. Therefore, the mean NDVI of each field was calculated for the period 2009–2017 using the shapefiles that define the fields. These average NDVI values were used to select six fields from both the model and standard farm for further analysis. Figure 4.2 visualized the mean values and shows which subset of fields were selected.

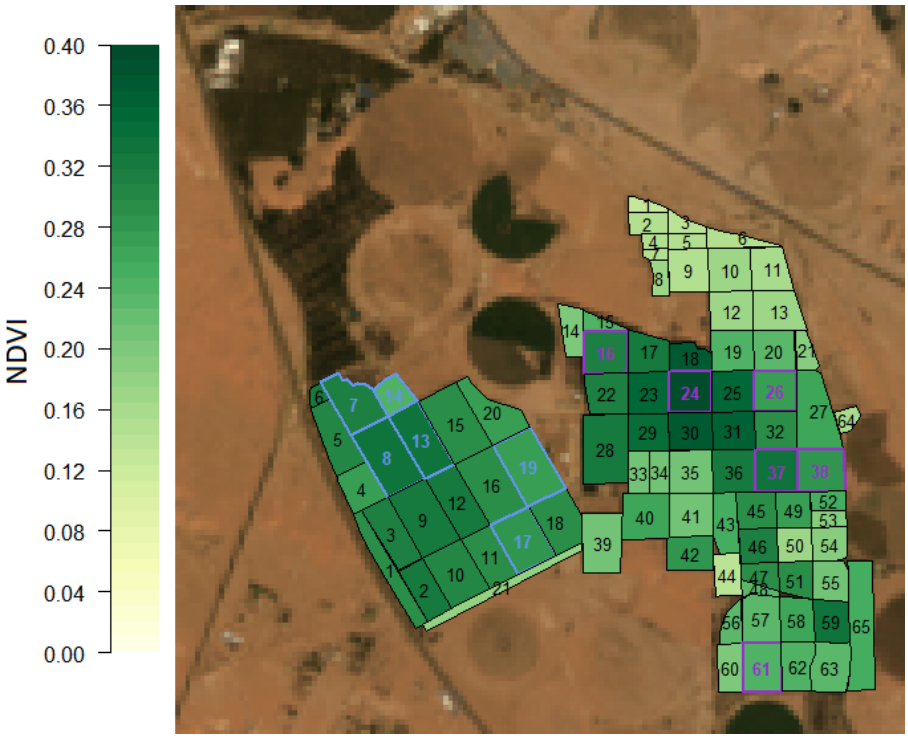

Figure 4.2: Map of average NDVI per date field, calculated from Landsat 7 imagery in the period 2009–2017. The selected fields for further analysis are highlighted with blue and purple for the model and standard plantations, respectively.

4.5 Interannual Trend Analysis

The NDVI values of the subset of fields were plotted against time to detect get insight in the NDVI development throughout the years and to identify if fields follow similar patterns or have offsets. LOESS trend lines were added to the scatter plot to make the different patterns better visible. To observe whether the detected signal is sensitive to

weather influences, precipitation and maximum daily temperature values were added to the plots. The meteorology data that was used for this is described in more detail in section 3.2.2. The precipitation was aggregated to 16-day sums, so the values indicate the total amount of rain that fell between two satellite passes. These plots were made for both the model and the standard farm to identify differences that are caused by the different farming techniques.

The interanual trend was also plotted in a map, similar to Figure 4.2. This was done to make the trend easily interpretable and make it possible to detect spatial correlations. The trend of all fields of both plantations was calculated by fitting a linear model, with formula $NDVI = a * time + b$, through the NDVI values. The slope parameter, a, in the model represents the change in NDVI per year and determined the colours of the polygons in the map. This map was also part of the fourth research question.

4.6 Seasonal Pattern Analysis

The average seasonal NDVI patterns of both farms were constructed to determine if different fields show phenological differences throughout the growing season. For constructing the average cycle the acquisition dates of the images were chronologically ordered based on their months and days, but ignoring the years in which they were taken. The remaining day/month combinations and their corresponding NDVI values were then plotted in a scatter plot and LOESS trendlines were added to better visualize the patterns. The harvesting and weeding moments on the model farm were also highlighted in the figures to determine if these operations would be visible in the satellite derived NDVI signals. The management operation dates were taken from the farm calender that is discussed in section 3.2.3.

To demonstrate an application for the outcome of this analysis I created a map similar to Figure 4.2 that shows the NDVI deviation for a specific date. This deviation would be calculated as the difference between the mean field value and the expected NDVI according to the seasonal pattern. A negative deviation means that the field is doing worse than expected. Because this was only a visualization of a concept I manually adjusted some field colours.

4.7 Heterogeneity Analysis

The palm trees within a field are all of similar age and of the same species, so it can be hypothesized that the pixel values within a field are homogeneous. To investigate this I looked at within-field and between-field heterogeneity of the NDVI values. The within-field heterogeneity indicates the variability of the pixel values within a field, while between-field heterogeneity compares the mean NDVI values of each field and represents

their variability. To calculate heterogeneity, H, I used equation 4.2 from a paper by Lobell and Azzari (2017).

$$H = Y_{95} - Y_{avg} \tag{4.2}$$

where Y_{95} is the 95^{th} percentile value and Y_{avg} is the mean NDVI value. The within-field heterogeneity was calculated by applying equation 4.2 on the NDVI values of all the pixels within a field. The between-field heterogeneity was derived by first calculating the mean NDVI value of each field and then applying equation 4.2 on the means. To get a better insight into the variability within the entire plantations I used all the fields from the model farm for this analysis and expanded the standard plantation subset by including fields 22, 23, 25, 27, 28, 29, 30, 31 and 32. These fields were picked based on their high mean NDVI in Figure 4.2. The heterogeneity was calculated for every Landsat 7 image in the period 2009–2017, resulting in multiple within-field time series in the same plot, as well as the between-field time series. Only the LOESS trend lines were plotted to make the trends more clear. More information about the construction of LOESS trend lines can be found in section 2.2.2. The time series plot was used to compare the between- and within-field heterogeneity to determine whether the fields are as homogeneous as hypothesized, or that their differences are as large as the differences between the fields.

A map that shows the heterogeneity of each field is plotted, similar to Figure 4.2, to demonstrate how the heterogeneity can be used by plantation managers to identify fields that contain large NDVI variations.

5 Results

The results of this study are presented and described in this chapter. First the results of the investigation into which indicator is most suitable for the date plantation monitoring, and from which data source this is best derived. The following three sections present the results of the three time series analyses; interanual trend, seasonal pattern and heterogeneity within the fields. Each of these three sections start with the analysis of the time series for both the model and standard farm, and ends with a map that exemplifies how the analysis can be used by a farmer.

5.1 Plantation Performance Indicators

It was first determined which vegetation index is most suited for monitoring the performance of a date plantation. I investigated the Normalized Difference Vegetation Index (NDVI) for its popularity, and the Soil Adjusted Vegetation Index (SAVI) because of the presence of much high bare soil on date plantations. The mean NDVI and SAVI values of the year 2011 were calculated for a field in the model farm, using Landsat 7 imagery. These values are plotted together in Figure 5.1 to show the differences.

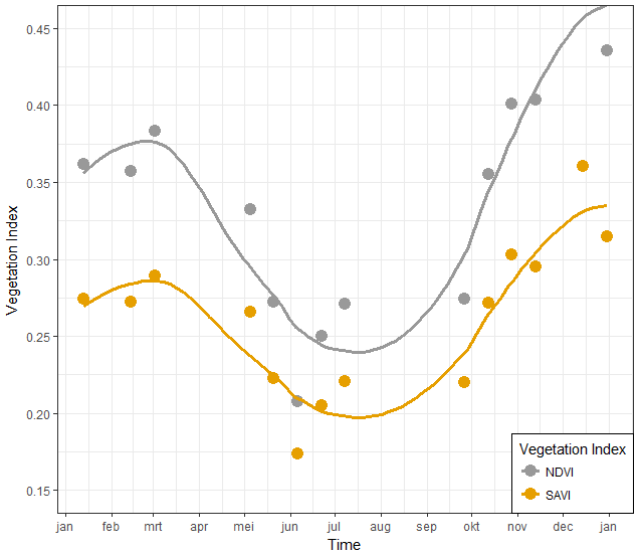

Figure 5.1: Mean NDVI and SAVI signals of Field 8 in the model farm. Values were calculated from Landsat 7 imagery of the year 2011.

Figure 5.1 shows one seasonal cycle of the date palms, visualized using two different vegetation indices. As explained in section 2.1 the palms prosper in the winter and experience water stress in the summer. This can be observed in both the NDVI and SAVI signals. No correlation could be made between the actual performance of the farms and a vegetation index, because there was no validation data available. Therefore, for the remainder of this study it was not important which signal showed the most accurate values. The main purpose of the vegetation index was to reveal differences and variations between fields and through time. Figure 5.1 shows a higher sensitivity to changes by NDVI as the range of values that is being used by NDVI signal is larger than that of SAVI. Therefore, the NDVI is used as the vegetation index for the remainder of this study. These observations also hold for other years and fields, which are presented in section B.1 of the Appendices.

For this research it was decided to use Landsat data for its high resolutions and long operational time. High spatial and temporal resolutions are needed to detect sub-field scale anomalies as soon as possible at the plantations, and multiple years of data are required to carry out the time series analysis. Both Landsat 7 and Landsat 8 meet these requirements, but it was uncertain whether their imagery would produce the same NDVI values as their sensors are slightly different. Their data could be used jointly if they produce the same output, reducing the revisit time from 16 to 8 days. Literature on this topic disagree; some studies conclude that no significant difference exists (Li, Jiang, and Feng 2013), while others find that NDVI from Landsat 8 data is consistently higher (Xu and Guo 2014; Flood 2014; Roy et al. 2016). Therefore, I calculated the NDVI values from both Landsat satellites and plotted their signals in the same graph to detect if a difference exists for date plantations (Figure 5.2).

The NDVI value distribution of both time series are shown as histograms in Figure 5.2 to support the time series. Similar figures that show the time series and histograms of other fields can be found in Appendix B.2.

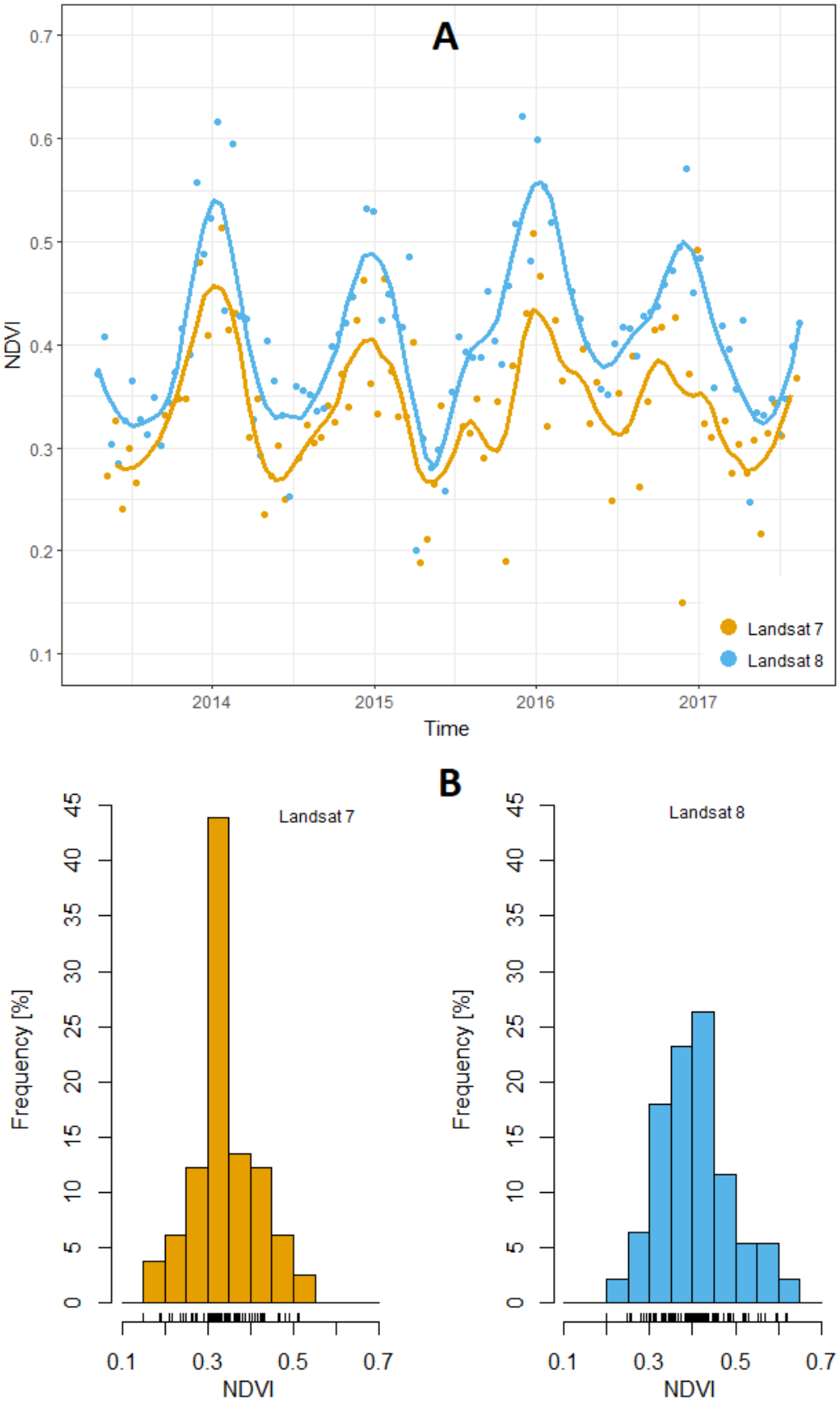

Figure 5.2: NDVI values calculated for Field 8 of the model farm using different satellites, Landsat 7 (orange) and Landsat 8 (blue). **A.** NDVI signals plotted against time and **B.** Histograms visualizing the NDVI value distribution.

The time series plot in Figure 5.2A shows that Landsat 8 derived NDVI values are consistently higher than those from Landsat 7. Both lines follow the same seasonal pattern but the peaks during the winters are larger for Landsat 8 imagery. The Landsat 7 signal shows multiple peaks in the autumns of 2015 and 2016. Figure 5.2B supports the observation that the NDVI values that are calculated from Landsat 7 imagery is consistently lower as the peak is at bin 0.3–0.35, whereas the peak of the Landsat 8 histogram is at bin 0.4–0.45. Because of this offset it was evident that the images of both satellites could not be used together unhindered. Literature on this topic suggests different solutions to correct for this offset, but investigating which one performs best was out of the scope of this research (Flood 2014; Roy et al. 2016). I decided to use only Landsat 7 imagery based on these results, because this satellite has been operational the longest and could therefore provide more data for the time series analysis.

5.2 Interannual Analysis

The first time series analysis was focussed on the interannual signal to determine if differences in the NDVI signals could be detected between the fields. The blocks in the farms contain different cultivars and are of different ages, and it was hypothesized that this would result in a different spectral response. The NDVI values were calculated for 6 fields from Landsat imagery of the years 2009–2017. The signals of the model farm fields are presented in Figure 5.3a and the standard farm fields are shown in Figure 5.3b. Precipitation data was also added to the plot to investigate whether variations in the signals can be explained by wet or dry weather.

Both Figure 5.3a and Figure 5.3b show a clear seasonality in the NDVI signals, with peaks during winter and dips in summer. However, trend lines are not fitted well through the high NDVI values in the winter. The signals of the model farm (Figure 5.3a) are close together, apart from field 14, which starts much lower but catches up after 2013. The signals of the standard farm (Figure 5.3b) are more separate from each other, with field 24 consistently having a much higher NDVI than the other fields. The management operations of the standard farm appears to be more irregular that the model farm, as the signals are less parallel and they vary much from year to year. The precipitation data shows that rainfall is irregular and inconsistent, both in timing and quantities, as some years hardly receive rain, while in 2013 there has been a very wet period. The largest precipitation peak was in the spring of 2013, when 46mm of rain fell within 16 days. Although this is much for an arid climate, it is equal to $4.6m^3$ for a large palm with a surface area of $10m^2$, which is half of what they typically receive in a month (Figure 3.2).

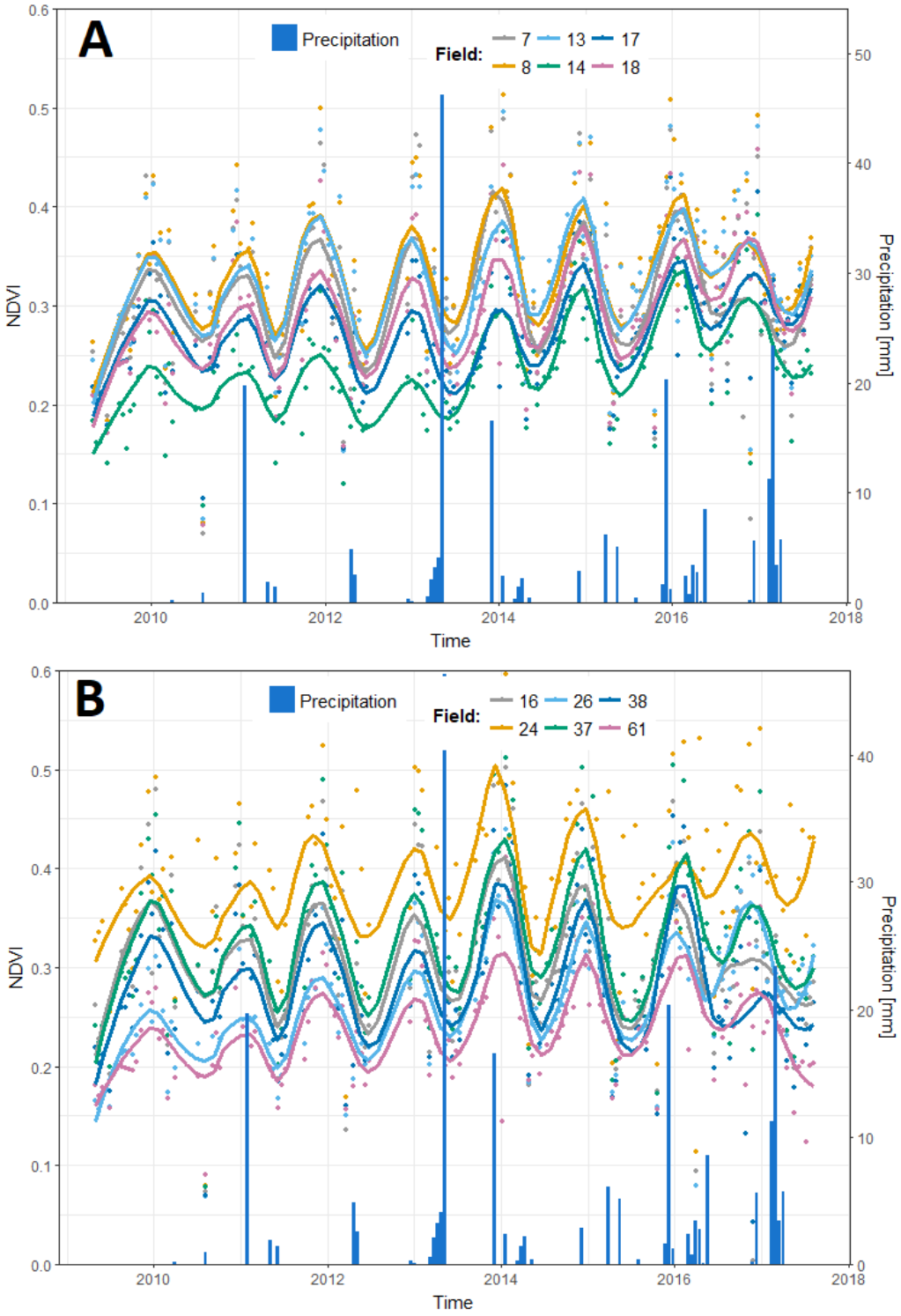

Figure 5.3: Interannual NDVI signals of 6 date fields plotted against the time, together with precipitation data (right axis). NDVI values calculated from Landsat 7 imagery for the period April 2009–August 2017. **A.** Model plantation. **B.** Standard plantation

Another weather variable that was hypothesized to potentially influence the date palm performance is the temperature, therefore the daily maximum temperature for the area is plotted in the same figure as the NDVI signals of the 6 fields on the model farm (5.4).

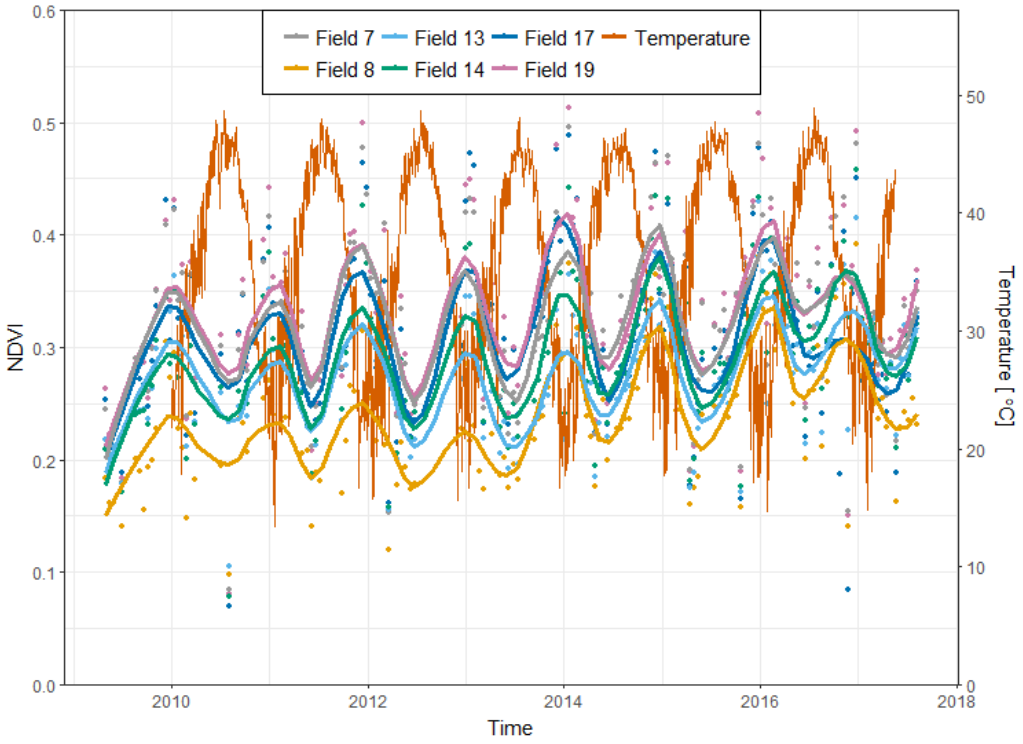

Figure 5.4: Interannual NDVI signals of 6 fields at the model plantation plotted against the time, together with the daily maximum temperature (right axis). NDVI values calculated from Landsat 7 imagery for the period April 2009–August 2017.

The temperature signal in Figure 5.4 is very consistent and regular. There is no year-to-year difference visible, but there is a little more day-to-day variation during the winter than during the summers. The temperature and NDVI signals are inversely correlated as the NDVI goes up when the temperature drops and vice versa. Higher temperatures result in more water stress, which reduces the chlorophyll activity that lowers the NDVI (Xiao and McPherson 2005). The same figure was made for the NDVI signals of the standard farm, but it did not contain additional information as the temperature cycle is so consistent. Therefore, this figure is presented in Appendix B.3.

Although Figures 5.3 and 5.4 show complete and detailed data about the farm, they do not provide accessible information for plantation managers. Therefore, I developed practical uses for the time series analyses outcomes, so they are more easily to utilize and interpret for everyone. The interannual signals were used to create a map that shows the interannual NDVI trend (Figure 5.5).

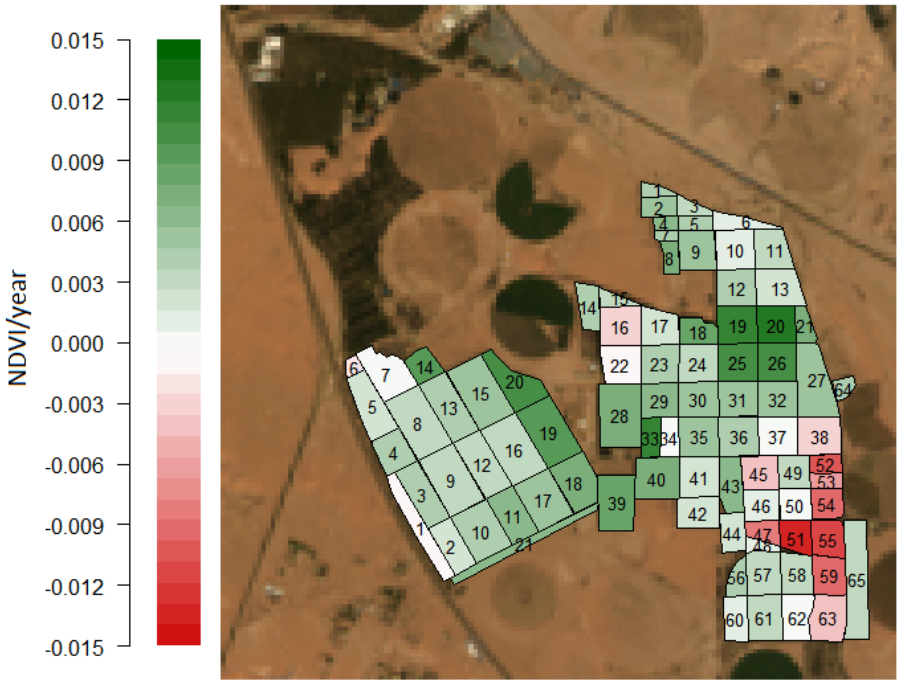

Figure 5.5: Interanual NDVI trend of the fields of the model farm (left) and the standard farm (right), obtained from fitting a linear model through the Landsat 7 NDVI values for the years 2009–2017.

Figure 5.5 shows for every field of the plantations the average NDVI increase or decrease over the period 2009–2017. From the map it is easy to identify which blocks gained NDVI, or what fields lost it. Furthermore, such a map can easily reveal spatial patterns. From Figure 5.5 it can be seen that the model farm had the largest NDVI increases in blocks 14, 19 and 20, and none of the fields had a NDVI decrease. The trends were more variable on the standard farm, with steep NDVI decreases for several fields in the southwest.

5.3 Seasonal pattern

The average yearly NDVI pattern of several fields is plotted in Figure 5.6 for the model farm and the in Figure 5.7 for the standard farm. These average patterns were constructed from all Landsat 7 imagery between 2009–2017 to get a more detailed pattern. It was hypothesized that some farm management operations could be detected in the signal, therefore also the weeding and harvesting periods are highlighted.

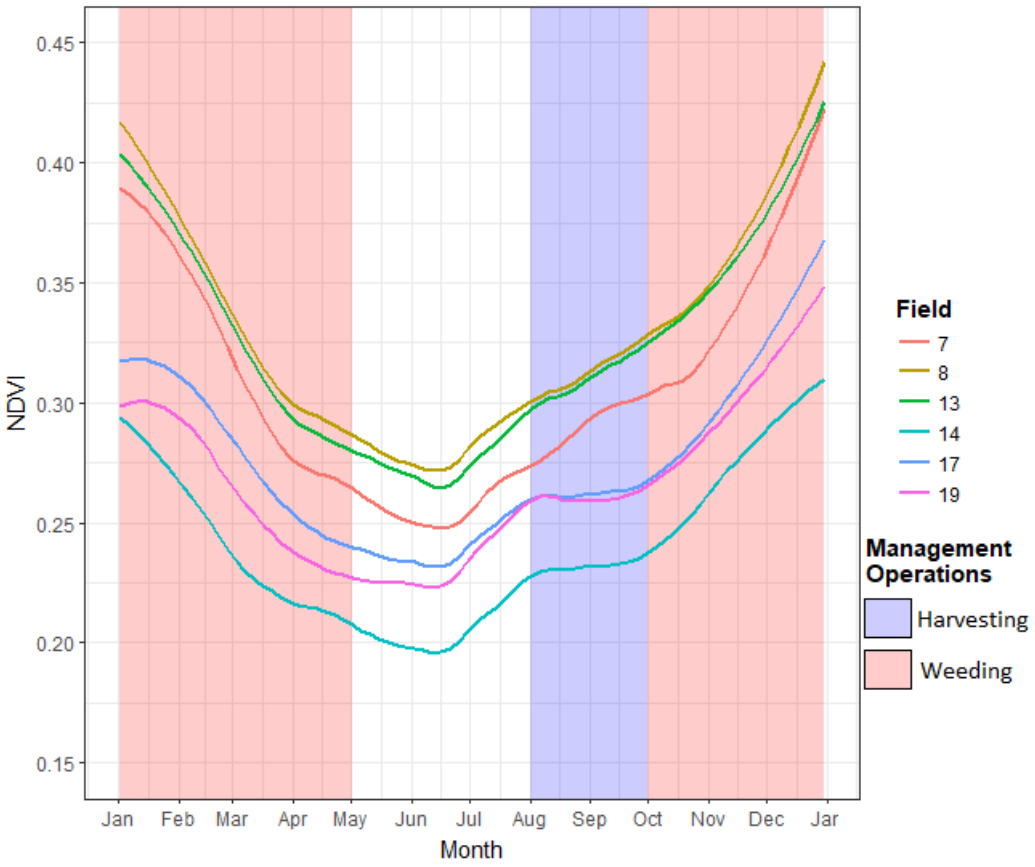

Figure 5.6: Average yearly NDVI signal of fields at the model plantation, calculated from Landsat 7 imagery between 2009–2017. The periods when weeding and harvesting occurs is highlighted red and blue, respectively.

Figure 5.6 shows that the average seasonal patterns of all fields have the same shape that run parallel to each other; high values in the winter and low NDVI values in the summer. However, the signals do differ in values as the lowest NDVI in June ranges between 0.20 and 0.28 for fields 14 and 8, respectively. Furthermore, the figure shows that weeding occurs in the months October – May, but this does not appear to affect the NDVI signal. Harvesting takes place in August and September, which appears to influence the signal as the NDVI increase stops after the summer.

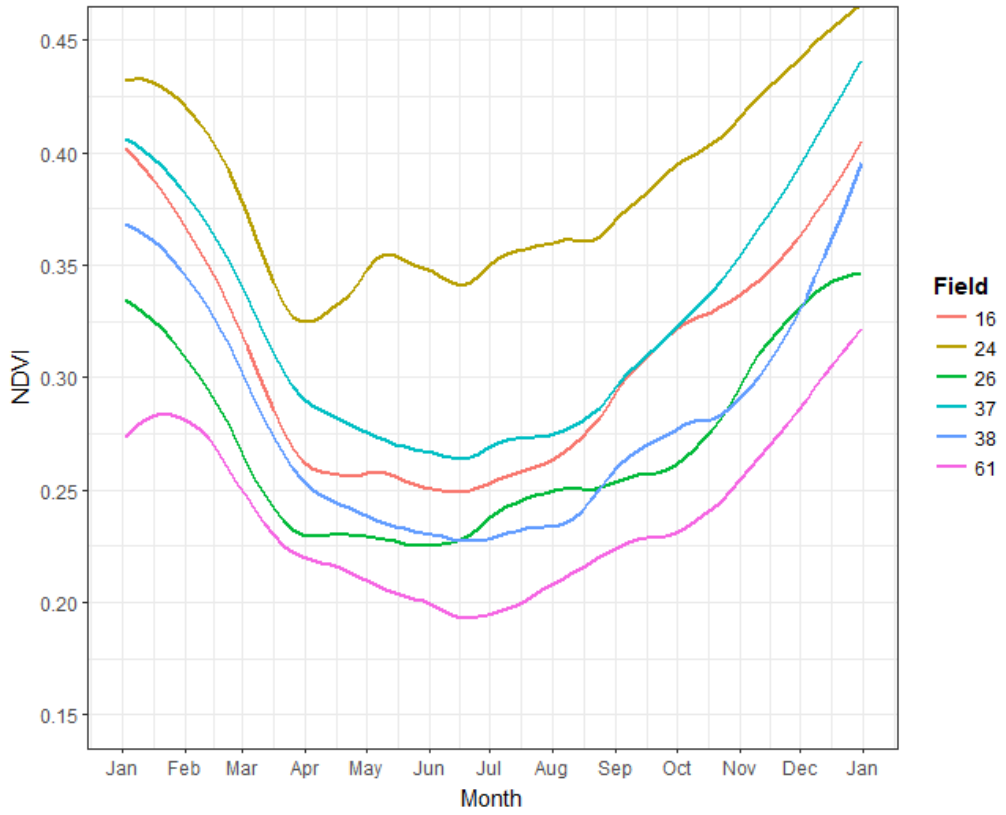

Figure 5.7: Average yearly NDVI signal of fields at the standard plantation, calculated from Landsat 7 imagery between 2009–2017.

The yearly NDVI patterns in Figure 5.7 shows a similar as the model farm for the standard farm, the NDVI is lowest in the summer and highest in the winter. However, the lines are much less parallel and have different shapes. The lines of fields 26 and 38 intersect three times and the dip in field 24 is not as deep as for the other fields. The large differences indicate that the fields within the standard farm are treated unequally, with large operations occurring in different months resulting in the fluctuating signals.

A map of the plantations was constructed again to implement the outcomes of the seasonal time series analysis in an accessible manner. In this application the latest observed values are compared with the average pattern (Figure 5.8). The resulting map can be used to see which fields are performing better or worse than they usually do, in terms of NDVI.

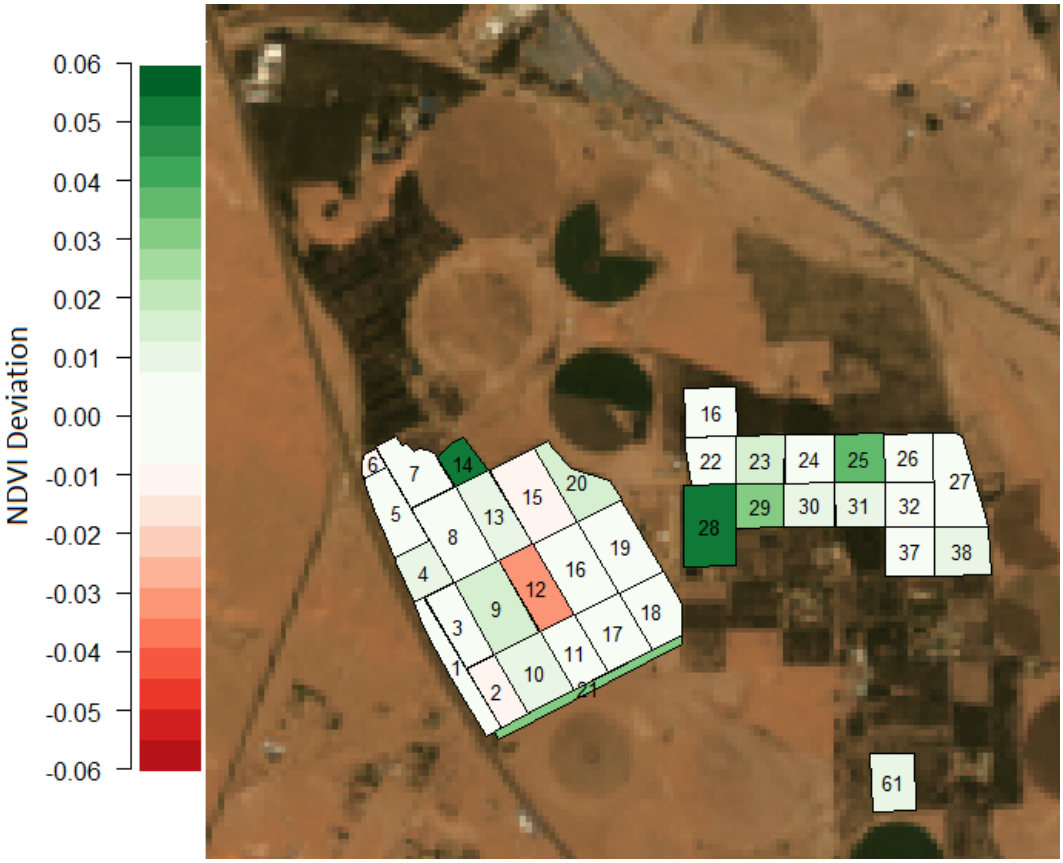

Figure 5.8: Deviation of the NDVI signal from the average seasonal pattern. Note that this is not an actual situation, but an artist impression.

Figure 5.8 does not show an actual situation so its application can be demonstrated. In the map it can instantly be seen that field 14 on the model farm and 28 of the standard farm are performing better than expected, whereas field 12 on the model farm is behind on its typical cycle. Therefore, based on this map it would be advised to investigate this field more closely.

5.4 Heterogeneity analysis

The within-field heterogeneity is a measure of the NDVI variability between the pixels within a field. Consequently, homogeneous vegetation results in low values and high values means that there are large NDVI differences between the pixels. Between-field heterogeneity indicates how much variability there is between the mean values of the fields. The within- and between-field heterogeneity were plotted together to investigate how they compare to each other. The heterogeneity of the model and standard plantations are presented in Figure 5.9 and Figure 5.10, respectively.

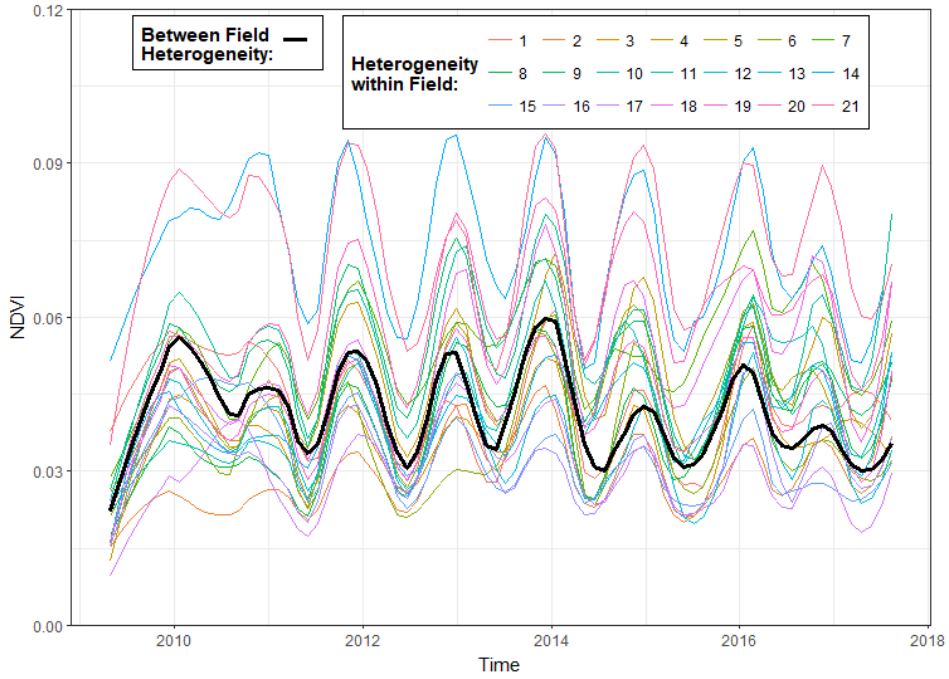

Figure 5.9: Within-field and between-field NDVI heterogeneity at the model farm, calculated from Landsat 7 imagery of the years 2009–2017.

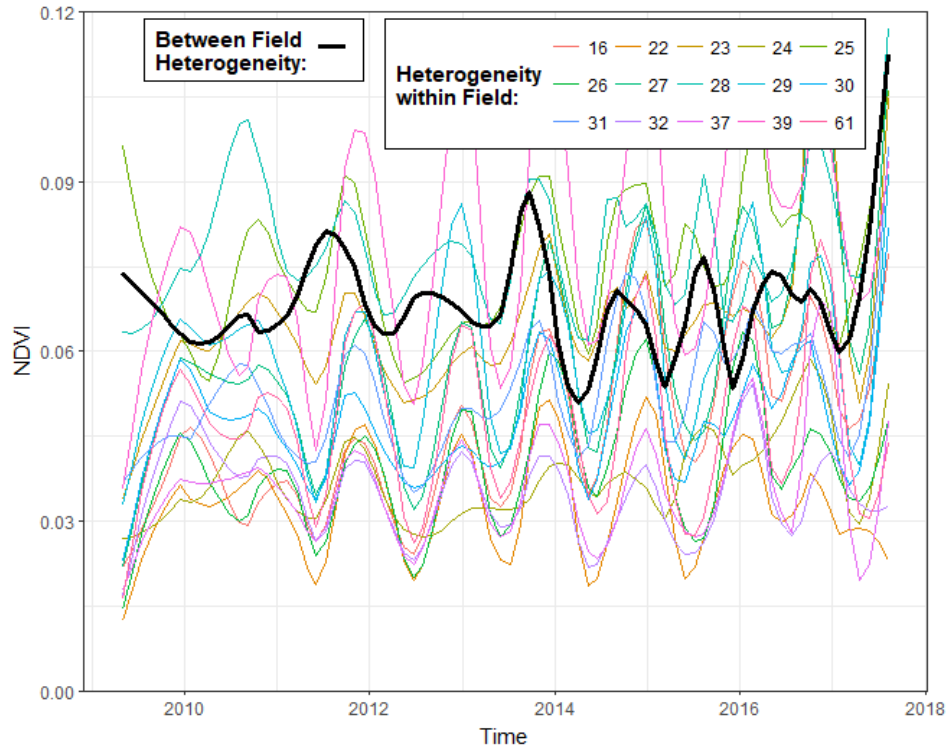

Figure 5.10: Within-field and between-field NDVI heterogeneity at the standard farm, calculated from Landsat 7 imagery of the years 2009–2017.

All fields in Figure 5.9 show a seasonal cycle, with most within-field heterogeneity in autumn, while the fields are most homogeneous in the spring and early summer months. This is also visible for the between-field heterogeneity. The values of both the within- and between-field variability range between 0.02–0.07, except for fields 14 and 17, which are consistently higher. Furthermore, the lines of all fields have similar shapes as they run more or less parallel.

Figure 5.10 shows that the shape of the heterogeneity signals of some fields have a seasonal cycle and are similar to those in Figure 5.9, but other fields have a different behaviour, resulting in many intersecting and tangled lines. The values range between 0.02–0.09 and the between-field heterogeneity varies around 0.07, which is higher than most of the within-field variability. This is also higher than the between-field heterogeneity of the model farm, indicating that the differences between the fields are larger. Furthermore, the shape of the between-field heterogeneity signal is very irregular and changes a lot from year to year. This can indicate that the farm management operations are not carried out the same each year.

An application was developed to make this information easier to interpret and use for farmers. Figure 5.11 visualizes the NDVI heterogeneity of each field in a map using a colour scale, calculated from an image that was taken at 2011-10-12. A farmer could use a map that was created from the latest image to identify heterogeneous fields. This indicates that not every date palm within that field is performing at the same level, which can be a reason for concern. From Figure 5.11 it can be concluded that field 7, 14 and 21 of the model farm, and field 25 and 28 of the standard farm are subject to heterogeneous vegetation.

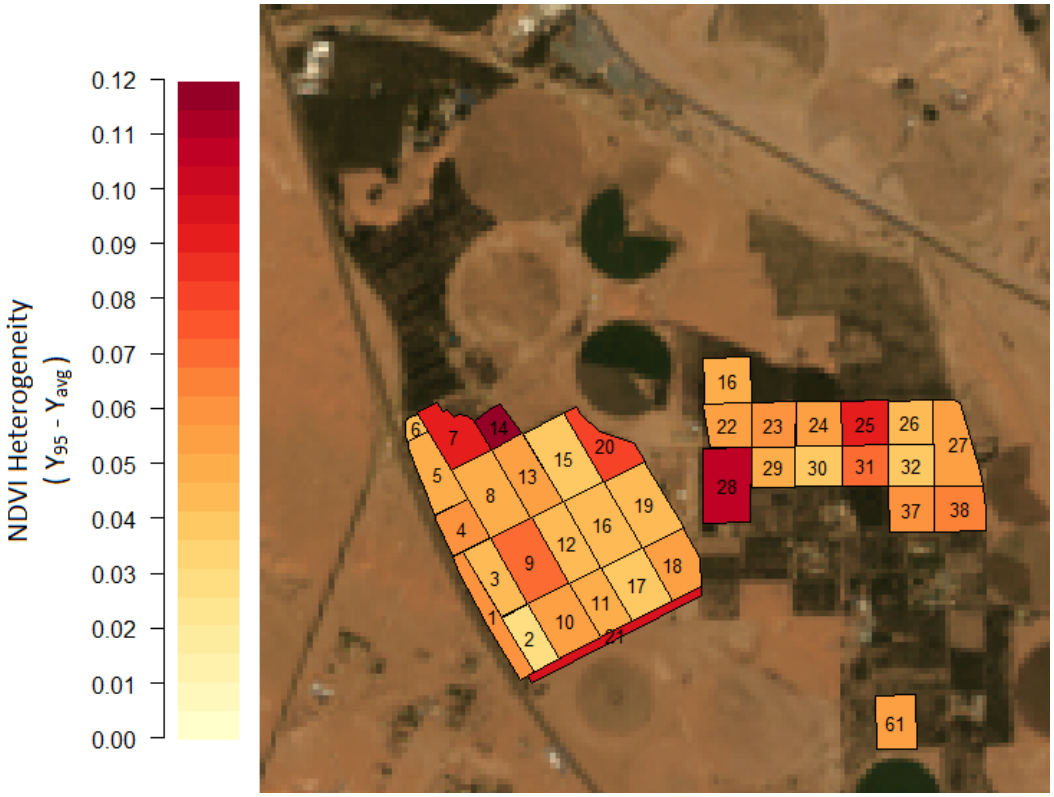

Figure 5.11: Heterogeneity of the NDVI values within each field, calculated as the difference between the mean and 95th percentile value. Calculated from a Landsat 7 image that was acquired at 2011-10-12.

6 Discussion

In this chapter the methods and results are discussed and interpreted by comparing them with existing scientific literature. The sections in this chapter have the same structure as the Results chapter, so the plantation performance indicators are discussed first, followed by a separate chapter for each time series analysis that was performed. Then a section discussing the potential for regional date monitoring, using satellite imagery. The last section also covers the discussion of the maps that were created to visualize the outcomes of the analyses in an accessible way.

6.1 Plantation Performance Indicators

The first research question can be split into two questions; what vegetation index is the best suited and what LandSat data is best suited for date plantation monitoring. I looked at two vegetation indexes to answer the first part, namely the popular NDVI (Normalized Difference Vegetation Index) and SAVI (Soil Adjusted Vegetation Index). SAVI was chosen because it was hypothesized that an index that compensated for bare soil would perform better in this case, as date palms are growing isolated and probably much bare soil is being detected. This reasoning is in line with Alhammadi et al (2008), who also used SAVI to study date palms. From this research we can conclude that NDVI values are consistently higher than SAVI values and follow similar trends (Figure 5.1). The comparable trends can be explained by the shared usage of the Red and NIR bands. Using a vegetation index that utilizes other bands, such as the Enhanced Vegetation Index (EVI), would likely show more differences. Literature finds that using SAVI produces more realistic values for low vegetation cover (Rondeaux, Steven, and Baret 1996; AR Huete 1988) and Bader et al (2013) found that the SAVI estimates can be improved by using a different soil bright correction factor. Nonetheless, NDVI is more suited for monitoring date plantations than SAVI because of its higher sensitivity. Other vegetation indices could have yielded better estimates of the greenness, but were not investigated in this study. Vegetation indices that can be particularly interesting are methods that utilize the new red-edge bands that the Sentinel-2 satellites provides, such as the red-edge chlorophyll index ($CI_{red-edge}$) and green chlorophyll index (CI_{green}) (Gitelson, Gritz, and Merzlyak 2003). These indices have been found to perform using Sentinel-2 imagery (Clevers and Gitelson 2013).

The second part of the first research question was aimed at investigating whether the NDVI values from LandSat 7 (LS7) and LandSat 8 (LS8) could be used collectively. Because of their different orbits it is not possible to have images of the same place and time from both satellites for comparison, but their differences can be seen by plotting their time series in the same graph (Figure 5.2a). The differences in trend, e.g. the double peaks in the Landsat 7 trend line, can be explained by atmospheric variation. For example, a sand storm or thin clouds that result in unusual low NDVI values, forcing the trend line to go down into a dip. Because the Landsat 7 and Landsat 8 values were always taken 8 days apart, these local variations can occur. Nonetheless, it can be concluded from this figure that LS8 values are substantially higher than LS7 for our data. The histograms of figure 5.2b confirm that this is not an artifact from the trend line construction. Literature disagree on the existence of this discrepency; some studies conclude that no significant difference exists (Li, Jiang, and Feng 2013), while others support my findings and state that NDVI from LS8 data is consistently higher (Xu and Guo 2014; Flood 2014; Roy et al. 2016). Xu et al (2014) found that the difference is larger for lower vegetation covers, explaining why a large difference is visible in this study. The discontinuity between LS7 and LS8 is found to be caused by a different spectral response from the two sensors, with greatest differences in the NIR and SWIR bands (Roy et al. 2016). Both Flood et al (2014) and Roy et al (2016) present statistical functions to overcome the difference. Roy et al. used ordinary least squares (OLS) regression to derive a linear transformation function and achieved r^2 values > 0.9. Flood et al. used orthogonal distance regression (ODR) to obtain a linear relation relation that reduced the difference to around 1%. However, I chose to not merge the data to avoid misinterpretations caused by transformation errors and only use LandSat 7 data because it has been longer operational. Nonetheless, it is possible that the results would have improved from merging the datasets, but investigating this was out of the scope of this study.

6.2 Interannual Analysis

The NDVI signals in Figure 5.3a and Figure 5.3b both show clear seasonal cycles, but the peaks and dips are not of the same magnitude every year. This indicates that variation between the seasons have been detected. These yearly variation appears to be influenced by the amount of precipitation, as both the standard and model farm have a higher peak after the excessive rainfall of 2013. However, the total amount of rain that was received by a palm tree of $10m^2$ during the large precipitation peak of 2013 was about half as much as it receives via irrigation in a month (Figure 3.2). Therefore, it is unlikely that the rainfall caused the NDVI peak. A possible explanation for the peak on the model farm can be the employment of the new plantation manager. His new approaches could have resulted in the higher NDVI values in the years 2014–2016. The standard farm

only shows one good year after the precipitation peak, which can possibly be explained by flourishing weeds after the heavy rainfall. Unfortunately, this is only speculation as there is no yield data available that could confirm or deny this hypothesis.

The NDVI signals of the model farm are more clumped than those of the standard farm, indicating that the fields are more similar on the model farm. The plot also shows the NDVI values that were derived from the satellite imagery. The trend line that was constructed did not fit well through the peaks in the winters. This can be solved by reducing the span parameter, but that also introduces noise to the line. Therefore, it is not advisable to compare the current state of a field with these interannual trend lines to monitor its performance, as they are mainly used for mutual comparisons. It is more advisable to use the seasonal pattern of the next section for this. Furthermore, the lines in Figure 5.3 are relatively parallel, implying that the inequality between fields is systematic, e.g. varying distances between the palms or very different species. Non-consistent NDVI differences between signals can be detected for field 14 for the model farm (Figure 5.3). The field is substantially less green up till 2013, after which it catches up with the other fields. This increase is also visible in Figures 4.2 and 5.5, which illustrates that field 14 has amongst the highest NDVI trends of the plantation, while having amongst the lowest average NDVI. The sudden change in performance coincides with the arrival of the new plantation manager, who may have noticed the relatively poor behaviour and addressed this successfully.

Figure 5.4 shows that the NDVI is inversely correlated with the temperature, because less chlorophyll is produced when the palms experience water stress (Xiao and McPherson 2005). Furthermore, there is less contribution to the greenness from weeds during the summer on the standard farm, as they are not as active in this period (Alhammadi and Glenn 2008). This is not an explanation for the model farm as they have a strict weeding regime. Figure 5.4 also shows that the yearly temperature development is very constant, meaning that its effect on the date palm growth is the same every year as well. Consequently, NDVI variations cannot be explained by temperature fluctuations.

6.3 Seasonal Analysis

The average seasonal patterns that are presented in Figure 5.6 and Figure 5.7 all have convex shapes, with lowest NDVI values in the summer and highest values in the winter. This is in agreement with earlier deductions and was attributed to a decrease in chlorophyll due to water stress in the hot summers (Xiao and McPherson 2005). The weeding moments on the model farm cannot be traced back in Figure 5.6, the resulting NDVI changes are too small and fade out in the convex seasonal shape. On the other hand, the harvesting moments align well with the breaks in the climbing NDVI signal. Thus, the removal of the date fruits result in a NDVI change that is substantial enough to be detected by the satellites.

The abnormal behaviour of field 24 of the standard farm can be seen in Figure 5.7 again. Seemingly, the NDVI decreases similar to the other fields, but suddenly increases again in April for no apparent reason. Another typical feature of the model farm is that fields 16 and 26 have similar patterns where the NDVI stops decreasing in April, while fields 61, 37 and 38 keep declining. I can only guess what the cause of this difference is without more in situ knowledge, e.g. the use of two different cultivars, or whether it is related to the behaviour of field 24.

6.4 Heterogeneity Analysis

The plots from Figure 5.9 and Figure 5.10 show how much heterogeneity in NDVI there is within each field, but also how much variability there is between the average values of the fields. Both the model and standard farm show a seasonality in their heterogeneity with most variability in the autumn–winter and least in the spring. This can be caused by pruning and frond cutting that happens in October–March (Figure A2 in Appendix A). Begue et al (2008) found that harvesting results in high heterogeneity when they studied within-field variability of sugarcane using SPOT NDVI time series. One part of the plantation has much of its leafs removed when the satellites passes, while the other part still has all of its leafs. Both the within- and between-field heterogeneity is substantially higher at the standard farm than at the model farm. Only fields 14 and 21 of the model farm show are really high compared to the others, which can be explained by mixed pixels due to their shapes. Figure 4.2 shows that field 14 is small and field 21 is very elongated, resulting in relatively more edge pixels. The between-field heterogeneity of the model farm falls well within the range of the within-field signals, meaning that there is as much vegetation variability within the fields as between them. Consequently, one would not be able to distinguish the different fields using the satellite NDVI data if there would be no roads between them, despite their different cultivars and ages. This is different for the standard farm where the average vegetation of the fields have a high variability between them, which is larger than the heterogeneity within the fields. Figure 4.2 supports these findings, as the NDVI differences in the map are also larger for the standard farm than the model farm.

6.5 Satellite Monitoring Potential

The interannual, seasonal and heterogeneity analyses have shown that much variability in the NDVI time series can be detected from satellite imagery. Unfortunately the variations cannot be linked to yield fluctuations or biomass estimates as this validation data was not available for this study. Nonetheless, other studies were considerably successful in estimating these properties for oil palm, showing potential for date palm applications (Balasundram, Memarian, and Khosla 2013; Dong et al. 2015). Morel et

al. (2011) attempted to estimate aboveground biomass of oil palm plantations using synthetic-aperture radar (SAR), but concluded that their estimates failed due to high precipitation amounts and moist air. However, this technique should work fine for date plantations as they are located in arid regions with little rain and dry air.

In this study I have presented three examples of date monitoring applications that could be implemented for aid the farmers, namely the NDVI trend map (Figure 5.5), the NDVI deviation map (Figure 5.8) and the NDVI heterogeneity map (Figure 5.11). These maps are easy to interpret and can therefore be used by farmers with little knowledge of time series analysis. These three maps can potentially be merged into one map that combines the information and visualized a more arbitrary unit, e.g. 'need for further inspection'. Using time series analysis, the historic data gives reliable expected patterns, especially because the arid climate is so stable and not much year-to-year variation should be expected. The low amount of cloudy and overcast days make satellite monitoring a very powerful tool that has great potential to aid modernization of the entire agricultural sector in the Middle-East.

Many improvements possible to enhance the performance. Firstly, the temporal resolution of the Landsat data can be doubled by merging the data, e.g. by using the methods proposed by Flood et al. (2014) or Roy et al. Roy et al (2016). Soon, the Sentinel-2 constellation will be operational for long enough to provide multiple years of even higher resolution data, and additional spectral bands that can be used for several other indices. To implement these monitoring systems on a regional level, the locations of all date plantations have to be known. If this is not the case, a classification step has to be included to automatically detect plantations, similar to the research by Dong et al. (2015) who detected oil and acacia plantations within rain forest.

7 Conclusions & Recommendations

This chapter features the conclusions that can be drawn from this study, which also answer the research questions. Furthermore, recommendations for future research on this topic is presented, followed by an acknowledgements section to thank everyone who made this study possible.

7.1 Conclusions

In order to provide date farmers in the middle-east with a new monitoring tool, I explored the potential of using Landsat satellite imagery to survey date plantations. I compared a modern 'model' and traditional 'standard' farm, and two vegetation indices. Furthermore, three time series analyses were performed to determine the interannual trend and average seasonal pattern of date fields, and heterogeneity within the fields. The research questions of this study are answered by drawing the following conclusions: (i) Landsat 7 NDVI signals are the most sensitive to vegetation changes and could not be used with Landsat 8 NDVI data. (ii) The NDVI signals of the different fields follow logical and distinct patterns. They also show interannual growth and harvesting operations are detectable. But the signals are unaffected by weeding, precipitation and temperature. (iii) Both farms are characterized by different types of time series; the model farm shows parallel and regular signals, whereas the standard farm is irregular and has large differences between the fields. (iv) To best aid the farmers it is essential to provide accessible information, therefore the time series analysis outcomes were visualized in clear maps.

7.2 Recommendations

The results of this study show that the LandSat 7 NDVI time series are sensitive to vegetation changes. However, validation data is required to determine whether the NDVI variation correlate with biomass or yield fluctuations. Therefore, it is recommended that for additional research one must obtain yield data, preferably at field-level, to support the observations. Furthermore, it would be very helpful for interpretation of the results to have more knowledge of the plantations, the traditional farm in particular. Knowing the differences between the fields, e.g. about the cultivars, ages, special treatment, can help

make the connection between the NDVI signal and the story behind it. Therefore, it is recommended for further research to be able to communicate directly to preferably both plantation managers. Future research should also investigate the potential of Sentinel-2, as the satellites will be operational for long enough to be used for time series analysis. It would be very valuable if eventually the data of different satellites can be combined, e.g. Sentinel 1 & 2, Landsat 7 & 8 etc. Therefore, more research into data fusion is also recommended.

Acknowledgements

I would like to take this opportunity to thank several people without whom this study would never have been possible. First of all, I thank my supervisor Lammert Kooistra for being understanding, supportive and guiding during this project. Secondly, I thank Steven Wonink for his advice, interest and time, but also eLEAF in general for granting me the opportunity to learn more about working as a GIS-professional. I thank Laurens Bierens for providing me with the required meteorological and farm management data. Furthermore, I am grateful for all the coffee breaks and lunches with Bart. Last, but certainly not least, I could not have finished this thesis without the endless love and support of my girlfriend, Annemiek.

Bibliography

Abdul Salam, M and Suad Al Mazrooei (2006). "Crop water and irrigation water requirements of date palm (Phoenix dactylifera) in the loamy sands of Kuwait". In: *III International Date Palm Conference 736*, pp. 309–315.

Aldrich, Robert C (1975). "Detecting disturbances in a forest environment.[ERTS land use surveys]". In: *Photogrammetric Engineering and Remote Sensing* 41, pp. 39–48.

Alhammadi, MS and EP Glenn (2008). "Detecting date palm trees health and vegetation greenness change on the eastern coast of the United Arab Emirates using SAVI". In: *International Journal of Remote Sensing* 29.6, pp. 1745–1765.

Allbed, Amal, Lalit Kumar, and Priyakant Sinha (2014). "Mapping and modelling spatial variation in soil salinity in the Al Hassa Oasis based on remote sensing indicators and regression techniques". In: *Remote Sensing* 6.2, pp. 1137–1157.

Almutairi, Bader et al. (2013). "Comparative Study of SAVI and NDVI Vegetation Indices in Sulaibiya Area (Kuwait) Using Worldview Satellite Imagery". In: 1, pp. 50–53.

Al-Amoud, Ahmed I (2006). "Date palm response to subsurface drip irrigation". In: *2006 ASAE Annual Meeting*. American Society of Agricultural and Biological Engineers, p. 1.

Arias, Enrique, Alison Jane Hodder, and Abdallah Oihabi (2016). "FAO support to date palm development around the world: 70 years of activity". In: *Emirates Journal of Food and Agriculture* 28.1, p. 1.

Atwa, Atwa A and Esmat M Hegazi (2014). "Comparative susceptibilities of different life stages of the red palm weevil (Coleoptera: Curculionidae) treated by entomopathogenic nematodes". In: *Journal of economic entomology* 107.4, pp. 1339–1347.

Balasundram, Siva K, Hadi Memarian, and Rajiv Khosla (2013). "Estimating oil palm yields using vegetation indices derived from Quickbird". In: *Life Sci. J* 10.4, pp. 851–860.

Begue, Agnes, Pierre Todoroff, and Johanna Pater (2008). "Multi-time scale analysis of sugarcane within-field variability: improved crop diagnosis using satellite time series?" In: *Precision Agriculture* 9.3, pp. 161–171.

Bianchi, Marco, Martin Boyle, and Deirdre Hollingsworth (1999). "A comparison of methods for trend estimation". In: *Applied Economics Letters* 6.2, pp. 103–109.

Bolton, Douglas K and Mark A Friedl (2013). "Forecasting crop yield using remotely sensed vegetation indices and crop phenology metrics". In: *Agricultural and Forest Meteorology* 173, pp. 74–84.

Box, George EP et al. (2015). *Time series analysis: forecasting and control*. John Wiley & Sons.

Cai, Xiaobin et al. (2016). "Remote sensing of the water storage dynamics of large lakes and reservoirs in the Yangtze River Basin from 2000 to 2014". In: *Scientific reports* 6.

Chao, ChihCheng T and Robert R Krueger (2007). "The date palm (Phoenix dactylifera L.): overview of biology, uses, and cultivation". In: *HortScience* 42.5, pp. 1077–1082.

Chen, Xi C et al. (2013). "Contextual time series change detection". In: *Proceedings of the 2013 SIAM International Conference on Data Mining*. SIAM, pp. 503–511.

Chivasa, Walter, Onisimo Mutanga, and Chandrashekhar Biradar (2017). "Application of remote sensing in estimating maize grain yield in heterogeneous African agricultural landscapes: a review". In: *International Journal of Remote Sensing* 38.23, pp. 6816–6845.

Chong, Khai Loong et al. (2017). "A review of remote sensing applications for oil palm studies". In: *Geo-spatial Information Science* 20.2, pp. 184–200.

Cleveland, William S (1979). "Robust locally weighted regression and smoothing scatterplots". In: *Journal of the American statistical association* 74.368, pp. 829–836.

Cleveland, William S and Susan J Devlin (1988). "Locally weighted regression: an approach to regression analysis by local fitting". In: *Journal of the American statistical association* 83.403, pp. 596–610.

Clevers, Jan GPW and Anatoly A Gitelson (2013). "Remote estimation of crop and grass chlorophyll and nitrogen content using red-edge bands on Sentinel-2 and-3". In: *International Journal of Applied Earth Observation and Geoinformation* 23, pp. 344–351.

Cohen, Y et al. (2012). "Use of aerial thermal imaging to estimate water status of palm trees". In: *Precision Agriculture* 13.1, pp. 123–140.

Collins, John B and Curtis E Woodcock (1996). "An assessment of several linear change detection techniques for mapping forest mortality using multitemporal Landsat TM data". In: *Remote sensing of environment* 56.1, pp. 66–77.

Coppin, Pol R and Marvin E Bauer (1995). "The potential contribution of pixel-based canopy change information to stand-based forest management in the northern US". In: *Journal of Environmental Management* 44.1, pp. 69–82.

Corporation, Namibia Development (2018). *NDC Website - Homepage*. URL: `http://www.ndc.org.na/` (visited on 01/13/2018).

DeVries, Ben et al. (2015). "Robust monitoring of small-scale forest disturbances in a tropical montane forest using Landsat time series". In: *Remote Sensing of Environment* 161, pp. 107–121.

Dong, Xichao et al. (2015). "Feasibility study of C-and L-band SAR time series data in tracking Indonesian plantation and natural forest cover changes". In: *IEEE Journal of Selected Topics in Applied Earth Observations and Remote Sensing* 8.7, pp. 3692–3699.

ESA (2018). *ESA Copernicus Website - Overview*. URL: http://m.esa.int/Our_Activities/Observing_the_Earth/Copernicus/Overview4 (visited on 01/13/2018).

FAO (2012). *FAOSTAT Database, Rome*. URL: http://faostat3.fao.org/home/E (visited on 07/17/2016).

Fernandes, Jeferson Lobato, Nelson Francisco Favilla Ebecken, and Júlio César Dalla Mora Esquerdo (2017). "Sugarcane yield prediction in Brazil using NDVI time series and neural networks ensemble". In: *International Journal of Remote Sensing* 38.16, pp. 4631–4644.

Flood, Neil (2014). "Continuity of reflectance data between Landsat-7 ETM+ and Landsat-8 OLI, for both top-of-atmosphere and surface reflectance: a study in the Australian landscape". In: *Remote Sensing* 6.9, pp. 7952–7970.

Galford, Gillian L et al. (2008). "Wavelet analysis of MODIS time series to detect expansion and intensification of row-crop agriculture in Brazil". In: *Remote sensing of environment* 112.2, pp. 576–587.

Gazette, Saudi (2016). *Kingdom's groundwater 'will run out in 13 years'*. URL: http://www.arabianbusiness.com/saudi-groundwater-will-run-out-in-13-years--621171.html (visited on 12/25/2016).

Giblin-Davis, Robin M (2001). "Borers of palms". In: *Insects on palms. Edited by FW Howard, Moore, D, Giblin-Davis RM, Abad, RG. CABI Publishing, Wallingford, GB*, pp. 267–304.

Gitelson, Anatoly A, Yuri Gritz, and Mark N Merzlyak (2003). "Relationships between leaf chlorophyll content and spectral reflectance and algorithms for non-destructive chlorophyll assessment in higher plant leaves". In: *Journal of plant physiology* 160.3, pp. 271–282.

Gorji, Taha, Elif Sertel, and Aysegul Tanik (2017). "Monitoring soil salinity via remote sensing technology under data scarce conditions: A case study from Turkey". In: *Ecological Indicators* 74, pp. 384–391.

Goward, Samuel N et al. (2008). "Forest disturbance and North American carbon flux". In: *Eos, Transactions American Geophysical Union* 89.11, pp. 105–106.

Gush, H (1999). "Date with disaster". In: *The Gulf Today*, p. 16.

Gutiérrez, Abelardo et al. (2010). "Development of a bioacoustic sensor for the early detection of Red Palm Weevil (Rhynchophorus ferrugineus Olivier)". In: *Crop Protection* 29.7, pp. 671–676.

Haj-Amor, Zied et al. (2016). "Soil salinisation and irrigation management of date palms in a Saharan environment". In: *Environmental monitoring and assessment* 188.8, p. 497.

Huete, Alfredo et al. (2002). "Overview of the radiometric and biophysical performance of the MODIS vegetation indices". In: *Remote sensing of environment* 83.1, pp. 195–213.

Huete, AR (1988). "A SOIL-ADJUSTED VEGETATION INDEX (SAVI)". In: *REMOTE SENSING OF ENVIRONMENT* 25.3, pp. 295–309.

Al-Ibrahim, Abdulla Ali (1991). "Excessive use of groundwater resources in Saudi Arabia: Impacts and policy options". In: *Ambio*, pp. 34–37.

Iverson, Louis R., Robin Lambert Graham, and Elizabeth A. Cook (1989). "Applications of satellite remote sensing to forested ecosystems". In: *LANDSCAPE ECOLOGY* 3.2, pp. 131–143.

Johnson, Dennis V (2016). "Unusual date palm products: Prayer beads, walking sticks and fishing boats". In: *Emirates Journal of Food and Agriculture* 28.1, p. 12.

Jonsson, Per and Lars Eklundh (2002). "Seasonality extraction by function fitting to time-series of satellite sensor data". In: *IEEE transactions on Geoscience and Remote Sensing* 40.8, pp. 1824–1832.

Al-Karaki, Ghazi N (2013). "Application of mycorrhizae in sustainable date palm cultivation". In: *Emirates Journal of Food and Agriculture* 25.11, p. 854.

Li, Peng, Luguang Jiang, and Zhiming Feng (2013). "Cross-comparison of vegetation indices derived from Landsat-7 enhanced thematic mapper plus (ETM+) and Landsat-8 operational land imager (OLI) sensors". In: *Remote Sensing* 6.1, pp. 310–329.

Lobell, David B and George Azzari (2017). "Satellite detection of rising maize yield heterogeneity in the US Midwest". In: *Environmental Research Letters* 12.1, p. 014014.

Lobell, David B, David Thau, et al. (2015). "A scalable satellite-based crop yield mapper". In: *Remote Sensing of Environment* 164, pp. 324–333.

Meteoblue (2017). *Meteoblue - Model Information*. URL: `https://content.meteoblue.com/en/research-development/data-sources/weather-modelling/model-run` (visited on 12/27/2017).

Modaihsh, Abdullah S et al. (2015). "Evaluation of soil degradation in Al-Kharj center, Saudi Arabia using remote sensing". In: *Int. J. Remote Sens. Geosci* 4.2, p. 7.

Morel, Alexandra C et al. (2011). "Estimating aboveground biomass in forest and oil palm plantation in Sabah, Malaysian Borneo using ALOS PALSAR data". In: *Forest Ecology and Management* 262.9, pp. 1786–1798.

Al-Omran, Abdulrasoul M et al. (2016). "Hydrochemical characterization of groundwater under agricultural land in arid environment: a case study of Al-Kharj, Saudi Arabia". In: *Arabian Journal of Geosciences* 9.1, p. 68.

Prince, SD and WL Astle (1986). "Satellite remote sensing of rangelands in Botswana I. Landsat MSS and herbaceous vegetation". In: *International Journal of Remote Sensing* 7.11, pp. 1533–1553.

Ren, Jie, James B Campbell, and Yang Shao (2017). "Estimation of SOS and EOS for Midwestern US Corn and Soybean Crops". In: *Remote Sensing* 9.7, p. 722.

Robert, C (1975). "Evaluation of ERTS-1 data for forest and rangeland surveys". In:

Robinson, ML, Brian Brown, and C Frank Williams (2002). "The date palm in southern Nevada". In: *University of Nevada, Cooperative Extension*.

Rondeaux, Geneviève, Michael Steven, and Frédéric Baret (1996). "Optimization of soil-adjusted vegetation indices". In: *Remote sensing of environment* 55.2, pp. 95–107.

Rouse Jr, J_W et al. (1974). "Monitoring vegetation systems in the Great Plains with ERTS". In:

Roy, DP et al. (2016). "Characterization of Landsat-7 to Landsat-8 reflective wavelength and normalized difference vegetation index continuity". In: *Remote Sensing of Environment* 185, pp. 57–70.

Running, Steven W (1986). "Global primary production from terrestrial vegetation: Estimates integrating satellite remote sensing and computer simulation technology". In: *Science of the total environment* 56, pp. 233–242.

Sakamoto, Toshihiro et al. (2005). "A crop phenology detection method using time-series MODIS data". In: *Remote sensing of environment* 96.3, pp. 366–374.

Schmidt, Gail et al. (2013). *Landsat ecosystem disturbance adaptive processing system (LEDAPS) algorithm description*. Tech. rep. US Geological Survey.

Shendryk, Iurii et al. (2016). "Mapping individual tree health using full-waveform airborne laser scans and imaging spectroscopy: A case study for a floodplain eucalypt forest". In: *Remote Sensing of Environment* 187, pp. 202–217.

Tao, Fulu et al. (2006). "Climate changes and trends in phenology and yields of field crops in China, 1981–2000". In: *Agricultural and Forest Meteorology* 138.1, pp. 82–92.

Tech, Virginia (2018). *Department of Statistics website - Regression Models*. URL: `http://www.lisa.stat.vt.edu/?q=node/7517` (visited on 01/13/2018).

Toureiro, Célia et al. (2017). "Irrigation management with remote sensing: Evaluating irrigation requirement for maize under Mediterranean climate condition". In: *Agricultural Water Management* 184, pp. 211–220.

Turner, DP et al. (2007). "Scaling net ecosystem production and net biome production over a heterogeneous region in the western United States". In: *Biogeosciences Discussions* 4.2, pp. 1093–1135.

United Nations (2015). "Key Findings and Advance Tables." In: *World Population Prospects: The 2015 Revision*.

USGS (2018). *USGS Landsat Website - Missions Timeline*. URL: `https://landsat.usgs.gov/landsat-missions-timeline` (visited on 01/13/2018).

Veloso, Amanda et al. (2017). "Understanding the temporal behavior of crops using Sentinel-1 and Sentinel-2-like data for agricultural applications". In: *Remote Sensing of Environment* 199, pp. 415–426.

Verbesselt, Jan et al. (2010). "Detecting trend and seasonal changes in satellite image time series". In: *Remote sensing of Environment* 114.1, pp. 106–115.

Vermote, Eric, Chris Justice, et al. (2016). "Preliminary analysis of the performance of the Landsat 8/OLI land surface reflectance product". In: *Remote Sensing of Environment* 185, pp. 46–56.

Vermote, Eric, Didier Tanré, et al. (1997). "Second simulation of the satellite signal in the solar spectrum, 6S: An overview". In: *IEEE transactions on geoscience and remote sensing* 35.3, pp. 675–686.

Xiao, Qingfu and E Gregory McPherson (2005). "Tree health mapping with multispectral remote sensing data at UC Davis, California". In: *Urban Ecosystems* 8.3, pp. 349–361.

Xin, Qinchuan et al. (2013). "A production efficiency model-based method for satellite estimates of corn and soybean yields in the Midwestern US". In: *Remote Sensing* 5.11, pp. 5926–5943.

Xu, Dandan and Xulin Guo (2014). "Compare NDVI extracted from Landsat 8 imagery with that from Landsat 7 imagery". In: *American Journal of Remote Sensing* 2.2, pp. 10–14.

Al-Zahrani, KH et al. (2016). "Role of agricultural extension service in creating decision-making environment for the farmers to realize sustainable agriculture in Al-Qassim and Al-Kharj regions-Saudi Arabia". In: *JAPS, Journal of Animal and Plant Sciences* 26.4, pp. 1063–1071.

Zaid, A et al. (2002a). "Date Palm Cultivation (edited and compiled by A. Zaid), CHAPTER IV: Climatic Requirements of Date Palm." In: *Plant Production and Protection Paper no. 156, Rev. 1*.

— (2002b). "Date Palm Cultivation (edited and compiled by A. Zaid), CHAPTER VII: Date Palm Irrigation." In: *Plant Production and Protection Paper no. 156, Rev. 1*.

Zhang, Xin et al. (2016). "Crop Mapping Using PROBA-V Time Series Data at the Yucheng and Hongxing Farm in China". In: *Remote Sensing* 8.11, p. 915.

Zhou, Liming et al. (2001). "Variations in northern vegetation activity inferred from satellite data of vegetation index during 1981 to 1999". In: *Journal of Geophysical Research: Atmospheres* 106.D17, pp. 20069–20083.

Zohary D & Hopf, M (2000). *Domestication of plants in the Old World. The origin and spread of cultivated plants in West Asia, Europe, and the Nile Valley.* Oxford: Oxford University Press.

Appendices

A Plantation Calendar

MOHAMADIA FARM: DATES CALENDAR

Month	Operation	Instructions
January	Irrigation	10 times monthly (700-800 L) each time
	Fertilization	Inorganic fertilizers (NPK + TEs)
	Weeding	Weeding
	Pest Control	Protective spraying for control of scale insects and general pests (insecticide + fungicide +mineral oil) Continue RPW control program and finish protective spraying
	Pruning, cleaning and Takreeb	Leaf pruning and Takreeb
	Others	Irrigation network maintenance Raise soil around tree trunk (tardeem)
February-March	Irrigation	12 times / month 700-800 L every time).
	Fertilization	Inorganic fertilizers (NPK + TEs)
	Weeding	Weeding
	Pest Control	Continue RPW control program
	Pollination	Pollination and bagging; the following should be observed: Collect pollen pockets as soon they open and put in dry cold place and rotate daily until dry. Collect after 2-3 days in dry boxes (they should be mature, of good quality and should be properly handled) Pollination should be after Doha Close follow up of opening of female flowers One male against 15-25 females
	Pruning, cleaning and Takreeb	Leaf pruning and Takreeb continues
	Others	In March start removing and planting of offshoots Maintenance of Light traps
April	Irrigation	Irrigation 12 times/month (750-800 L every time)
	Fertilization	Inorganic fertilizers (NPK + TEs)
	Weeding	Weeding
	Pest Control	Spray against LDM and Date Mites
	Pollination	Finish pollination and by this month fruit set is complete
	Thinning	Fruit thinning
	Offshoots	Removing and planting of offshoots
	Others	Untie fruit stalks and remove paper bags (if used)
May	Irrigation	Irrigation 15 times/month (750-800 L every time)
	Fertilization	Inorganic fertilizers (NPK + TEs)
	Pest Control	Spray against date mites

Figure A1: Yearly schedule of management operations on the model farm. Part 1/3.

		Continue RPW control program
	Thinning and Tadeel	Thinning and Tadeel (tasneed) (together) Remove fruit stalks: Leave 8-14 fruit stalks / palm (one stalk / 8 fronds) Remove inside strands 'shamrookhs' (for selected varieties) For selected varieties: shorten strands 'Shamrookhs' (5 cm from end) leave one fruit stalk for every 8 fronds Fruit thinning
	Others	Cover fruit with nets against birds
June	Irrigation	Irrigation 15 times/month (750-850 L every time)
	Pest Control	Control of GDM and Ephestia Spray against mites (very active this month)
	Thinning	Fruit thinning, Tarkeez and bagging. Fruit bagging (Coloring and sugar conversion starts); while covering shake fruit bunch to allow dry and infested fruits to drop; also remove infertile fruits if not removed during 'Tadeel'.
	Offshoots	Removing and planting of offshoots
July	Irrigation	Irrigation 15 times/month (750-850 L every time),
	Pest Control	You may spray selected varieties against Ephestia
	Others	"Tarkeez" Treat and prepare warehouses to receive dates Prepare harvesting tools (ladders, buckets, scissors, cars, tools, tractors, trailers, packing cartoons, harvesting canvas, labor requirements etc.)
August – September	Irrigation	Irrigation 15 times/month (750-850 L every time) drops to 12 time in Sep.
	Harvesting	Harvesting of Rutab (Sukkari, Wanan, Sullaj (better price at this time!)
	Offshoots	In Sept start removing and planting of offshoots
October – November	Irrigation	Irrigation: 12 times every month at 700-800 L every time (3 times weekly)
	Fertilization	Inorganic fertilizers (NPK + TEs)
	Weeding	Weeding
	Pest Control	Resume RPW control program after harvest finish
	Pruning, cleaning and Takreeb	Cleaning old stalks and male flower pockets Cleaning basins, fronds base from dropped fruits, removing dead, diseased and dry fronds Start frond cutting and Takreeb and tree head cleaning
	Offshoots	Removing and planting of offshoots

Figure A2: Yearly schedule of management operations on the model farm. Part 2/3.

December	Irrigation	8 times every month at 700-800 L every time (2 times weekly)
	Fertilization	Add organic fertilizer + In organic fertilizers (NPK + TEs)
	Weeding	Weeding
	Pest Control	Protective spraying Control of inflorescence worms
	Pruning, cleaning and Takreeb	Cleaning young seedlings; Frond cutting and Takreeb
	Others	Raise tree basins according to tree age/development. Irrigation network maintenance Spines removal Review and evaluate last season and prepare timelines for next season

Figure A3: Yearly schedule of management operations on the model farm. Part 3/3.

B Additional Results

This appendix presents results that contain no new information compared to the figures that are already presented in the Results chapter.

B.1 NDVI versus SAVI

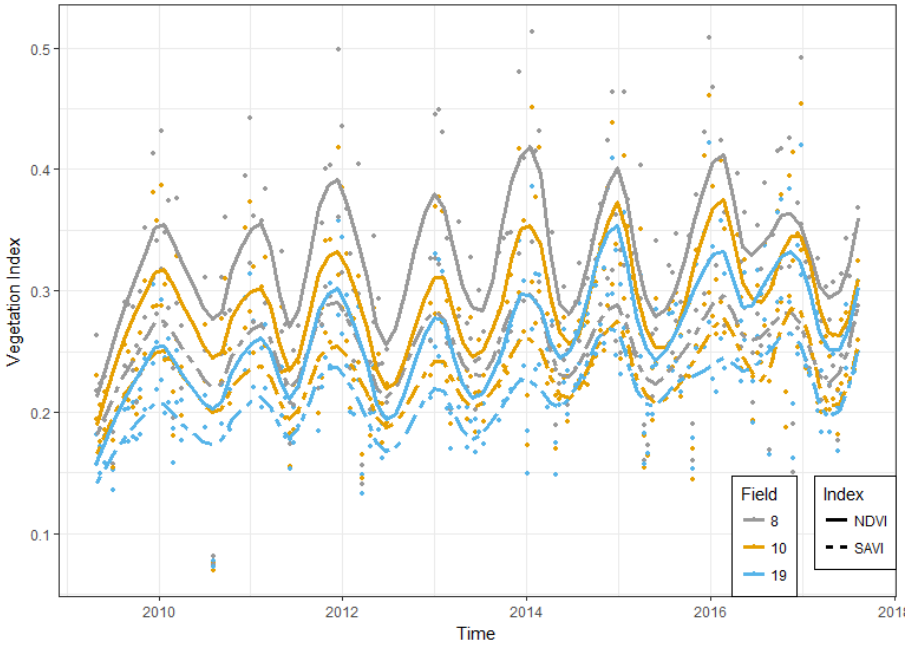

Figure B1: Mean NDVI and SAVI signals of Fields 8, 10 and 19 plotted against the time. Mean NDVI and SAVI signals of Fields 8, 10 and 19 were for calculated from Landsat 7 imagery between 2009–2017 and plotted against time.

B.2 LandSat 7 versus LandSat 8

NDVI signals calculated using different satellites for more fields of the standard farm, these plots are similar to Figure 5.2 in the Results chapter.

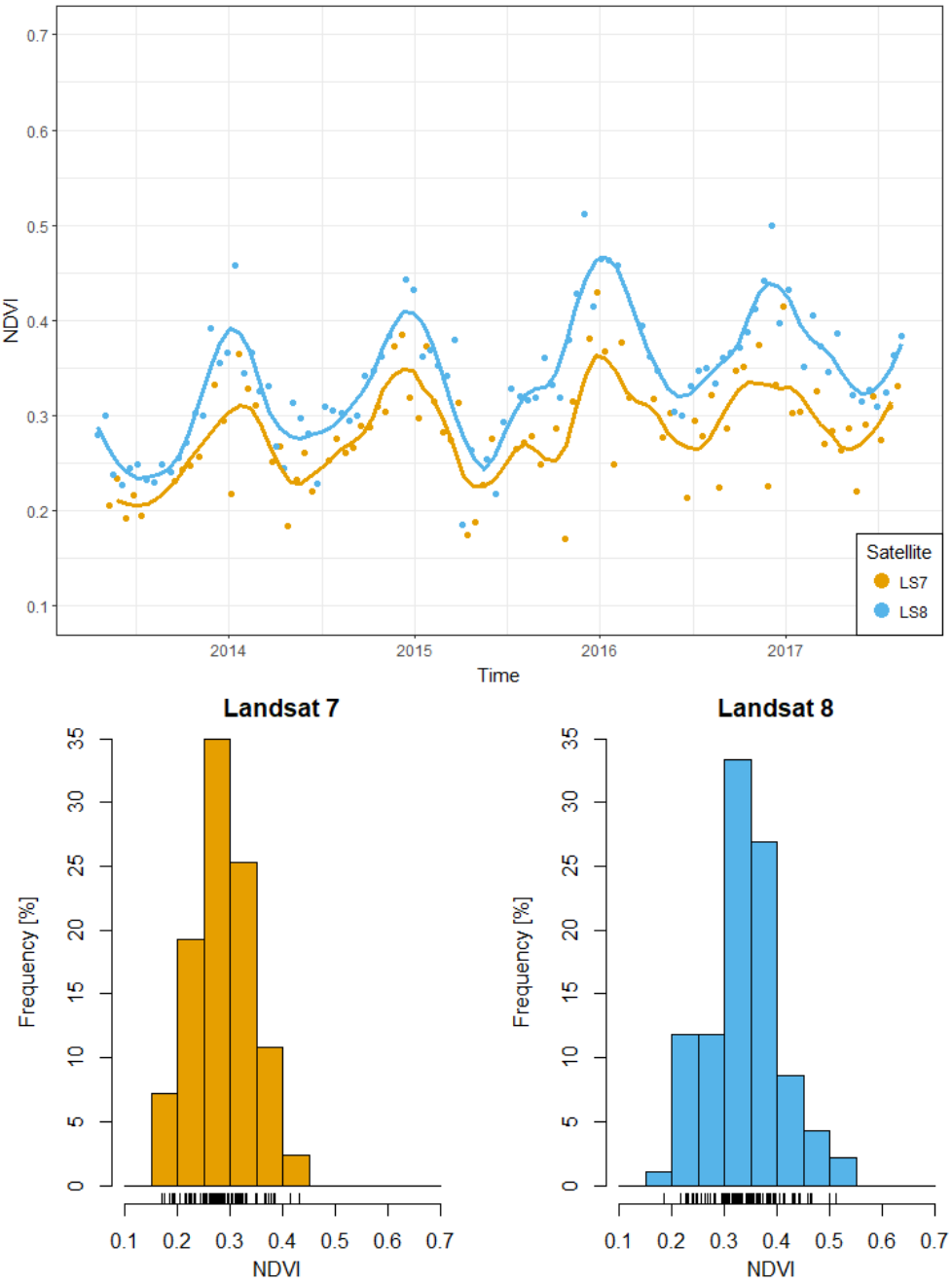

Figure B2: NDVI signals of field 17 of the model farm plotted against time (upper), calculated from LandSat7 (orange) and LandSat8 (blue). Histogram of the value distributions (lower).

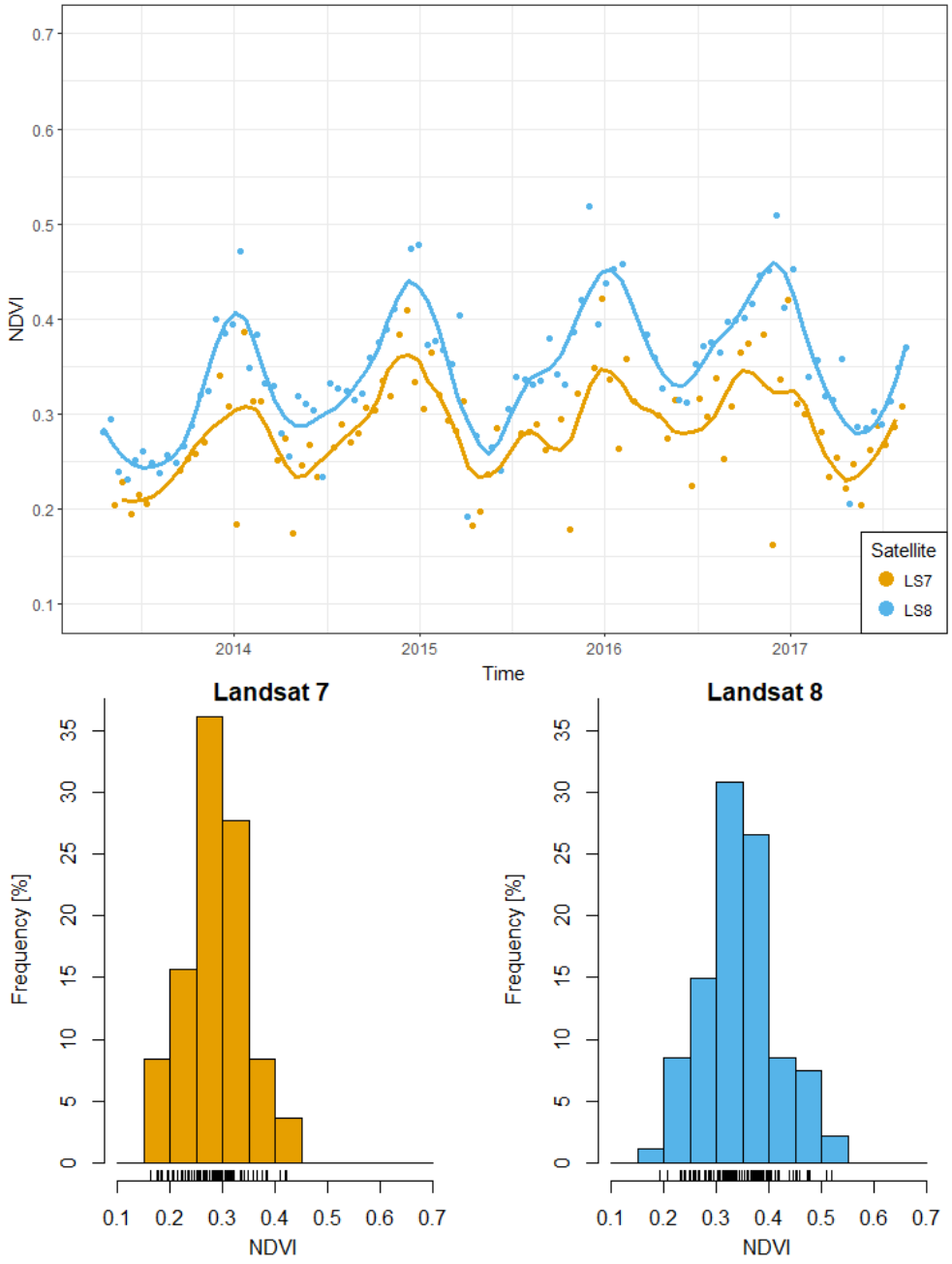

Figure B3: NDVI signals of field 19 of the model farm plotted against time (upper), calculated from LandSat7 (orange) and LandSat8 (blue). Histogram of the value distributions (lower).

B.3 Interannual Analysis

The interanual NDVI signals of fields in the standard farm are presented here, similar to Figure 5.4.

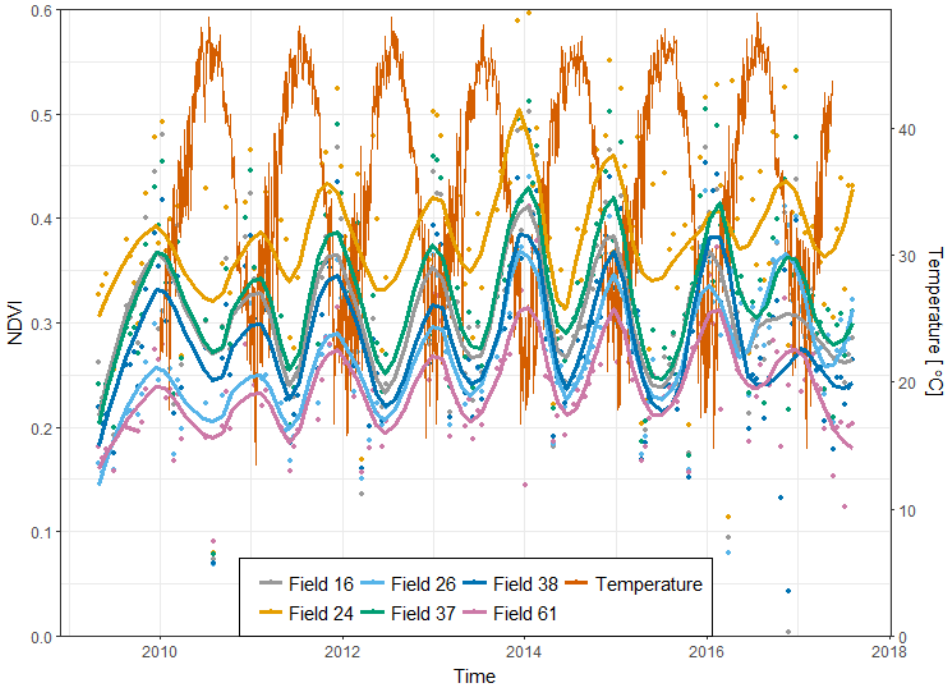

Figure B4: Interannual NDVI signals of 6 fields at the standard plantation plotted against the time, together with the daily maximum temperature (right axis). NDVI values calculated from Landsat 7 imagery for the period April 2009–August 2017

C USB Memorystick Content

The USB memorystick that accompanies this written report contains the following:

- Report (LaTeX files and PDF)
- Midterm and Final presentations (PPTX)
- Datasets used and created
- Scripts (R scripts)
- Literature (PDFs of used articles and Endnote)